The Function and Trafficking of Atg8 during Autophagosome Formation

by

Zhiping Xie

A dissertation submitted in partial fulfillment
of the requirements for the degree of
Doctor of Philosophy
(Molecular, Cellular, and Developmental Biology)
in The University of Michigan
2008

Doctoral Committee:

Professor Daniel J. Klionsky, Chair
Professor James Bardwell
Professor Robert S. Fuller
Associate Professor Amy Chang

To My Grandparents

Acknowledgments

First, I would like to thank my mentor Dr. Daniel J. Klionsky for giving me the privilege to work in his laboratory. I have learned invaluable lessons from not only his scientific expertise, but also from his passion towards scientific research and education. I am especially grateful for his enormous patience and openness as I explored through my oftentimes unorthodox experimental plans.

I would like to thank my thesis committee members, Dr. James Bardwell, Dr. Amy Chang, and Dr. Robert S. Fuller for their insightful suggestions and criticisms for my project. Additionally, I am grateful to Dr. Laura J. Olsen for her generous help at the beginning of my Ph.D. study. I would also like to thank Dr. Cumming Duan and Dr. James Bardwell for giving me the opportunities to do rotations in their laboratories, as well as Dr. Qijin Xu in the Duan laboratory and Dr. Jean-Francois Collet in the Bardwell laboratory for teaching me essential experimental techniques.

It has been wonderful to work together with members of the Klionsky laboratory. I would like to thank Dr. Hagai Abeliovich for his rigorous training that converted me from a spectator to an active participant in cell biology research. I also want to thank Dr. Per E. Stromhaug, Dr. Fulvio Reggiori and Dr. Takahiro Shintani for helpful advice in my research. I feel very fortunate to have Dr. Wei-Pang Huang, Dr. Usha Nair and Ms. Yang Cao as good friends. Furthermore, I thank all past and current labmates for providing a stimulating and comfortable environment.

I would also like to thank Dr. Edwards D. Rothman, Mr. Maciej B. Szefler and Mr. Ming-Jui Hsu for their assistance in statistics and computer programming, and Dr. Yanling Zhang for helpful discussions. Additionally, I am grateful for the people in the MCDB departmental office, in particular Ms. Mary Carr and Ms. Diane Durfy, for their constant assistance.

As I reflected on my academic endeavors during the writing of this thesis, from time to time my heart was filled with the memories of the people in the University of

Michigan. Here I would like to take the opportunity to express my gratefulness to all of you for making my life such a wonderful one despite the terrible stormy weather in Ann Arbor.

Finally, I would like to thank my family. I owe my gratitude to my grandparents and my parents. For so many years, they have nurtured me with unconditional and uninterrupted love and care. They will always be my source of inspiration. Last, but not least, I want to thank Dr. Qingqiu Gong for her love, encouragement and support.

Chapter 1 is reprinted from "Xie Z, Klionsky DJ. Autophagosome formation: core machinery and adaptations. Nat Cell Biol 2007; 9:1102-9" with minor modifications.

Chapter 2 is reprinted from "Xie Z, Nair U, Klionsky DJ. Atg8 controls phagophore expansion during autophagosome formation. Mol Biol Cell 2008; in press" with minor modifications. The electron microscopy sample preparation and image acquisition in Fig. 2.2A were performed by Dr. Usha Nair, Dept. of Molecular, Cellular and Developmental Biology, University of Michigan.

The R program code simulating the sectioning of vesicles in Chapter 3 was written by Mr. Maciej B. Szefler under the guidance of Dr. Edward D. Rothman, Dept. of Statistics, University of Michigan.

The analysis of the trafficking of Atg9 in Fig. 4.3A and the analysis of Atg8 localization in Figure 4.4 were performed by Ms. Yang Cao, Dept. of Molecular, Cellular and Developmental Biology, University of Michigan.

Table of Contents

List of Figures

List of tables

Abstract

Eukaryotic cells rely on autophagy to remove excess or damaged organelles and proteins. In this pathway, cytoplasmic materials are delivered to the lysosomes via double-membrane vesicles, the autophagosomes. The formation of autophagosomes, which involves the expansion and deformation of the precursor membrane sac, the phagophore, is catalyzed by the core autophagy machinery proteins at the phagophore assembly site (PAS). Previous studies have gradually discovered the order of assembly of the core autophagy machinery proteins at the PAS. In contrast, we know little about what these proteins do after PAS assembly. In this study, I first focused on how Atg8, one of the core machinery proteins, functions in autophagosome formation and demonstrated that (1) the amount of Atg8 at the PAS controls the size of autophagosomes produced and that (2) each round of autophagosome formation involves the recruitment of Atg8 to the phagophore and the subsequent deconjugation and release of Atg8 from this site. By tracing the trafficking of Atg8 in live cells, I established a temporal dissection of the autophagosome formation process. This allowed the examination of events at late stages of autophagosome formation and led to the further discovery that defects in Atg8 release not only arrest the existing autophagosome formation processes, but also prevent the regeneration of the PAS, which is necessary for sustained autophagosome formation. In addition, the data suggest that the release of Atg8 happens after the departure of Atg9 from the PAS, and that deconjugation of Atg8 is important in maintaining its correct localization. Furthermore, I developed two statistical methods for calculating the sizes of intracellular vesicles from sizes of their sections obtained through transmission electron microscopy. The methods were used to estimate the size of autophagic bodies, which is used in turn to estimate the area density of Atg8 molecules on the phagophore.

Chapter 1
Introduction: Core Molecular Machinery and Auxiliary Factors in Autophagosome Formation

Abstract

Eukaryotic cells employ autophagy to degrade damaged or obsolete organelles and proteins. Central to this process is the formation of autophagosomes, double-membrane vesicles responsible for delivering cytoplasmic material to lysosomes. In the past decade many autophagy-related, *ATG*, genes have been identified that are required for selective and/or nonselective autophagic functions. In all types of autophagy, a core molecular machinery plays a critical role in formation of the autophagosome. Additional auxiliary components allow autophagy to adapt to the changing needs of the cell.

Overview of autophagy

Eukaryotic cells employ autophagy, a potent lysosome-dependent mechanism of intracellular degradation, to eliminate objects ranging from soluble proteins to entire organelles under starvation or certain developmental and pathological conditions[1]. In multi-cellular organisms, autophagy has important roles in development, immune defense, programmed cell death, tumor suppression, and prevention of neuron degeneration[2-4].

Several forms of autophagy have been observed, including macroautophagy, microautophagy[5], chaperone-mediated autophagy[6] and piecemeal microautophagy of the nucleus[7①]. Here I focus on the most widely studied and potentially the most powerful one, macroautophagy (hereafter referred to as autophagy). In this pathway, an expanding membrane sac termed the phagophore enwraps portions of the cytoplasm (Figure 1.1). This leads to the formation of a double-membrane-bound, sequestering vesicle, called the autophagosome. Autophagosomes subsequently fuse with lysosomes, exposing their inner compartment to lysosomal hydrolases. The inner membrane of the autophagosome, together with the enclosed cargo, is then degraded, and the resulting molecules are released into the cytosol through lysosomal membrane permeases for recycling.

During the past decade, genetic screens in the yeast *Saccharomyces cerevisiae* and in other fungi have led to the isolation of individual gene products that participate in autophagy. To date, independent genetic screens in yeast model systems have identified 30 AuTophaGy-related (*ATG*) genes, which are involved in various subtypes of macroautophagy, including starvation-induced autophagy, the cytoplasm-to-vacuole targeting (Cvt) pathway and pexophagy[8]. Furthermore, orthologues of many yeast *ATG* genes have been identified in other eukaryotic organisms[8]. The characterization of these gene products have enriched our knowledge of the process, providing us with genetic and biochemical tools for exploring the diverse functions of autophagy under different physiological conditions and further deciphering the molecular mechanism of autophagy.

---

① Microautophagy involves direct uptake of cytoplasm at the lysosome surface by invagination of the limiting membrane of the lysosome. Chaperone-mediated autophagy also takes place at the lysosome membrane, but relies on translocation of unfolded proteins across the membrane. Piecemeal microautophagy of the nucleus is a selective type of autophagy that occurs in yeast that is used to degrade portions of the nucleus by taking them into the vacuole (the yeast analogue of the lysosome) lumen.

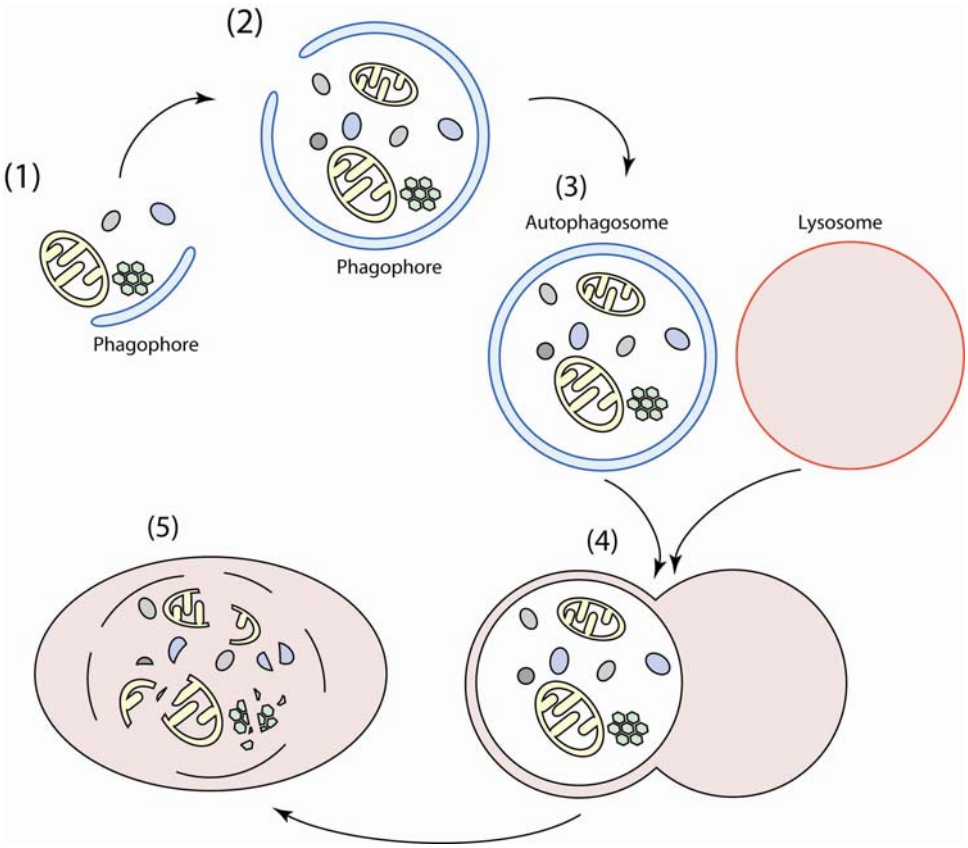

Figure 1.1 Schematic depiction of autophagy

Cytosolic material is sequestered by an expanding membrane sac, the phagophore (1, 2), resulting in the formation of a double-membrane vesicle, an autophagosome (3); the outer membrane of the autophagosome subsequently fuses with a lysosome, exposing the inner single membrane of the autophagosome to lysosomal hydrolases. (4); the cargo-containing vesicle is lysed, and the contents are degraded (5).

Core molecular machinery of autophagosome formation

Among the *ATG* genes, a subset of genes is required for autophagosome formation in all subtypes of autophagy. We refer to the corresponding gene products as the 'core' autophagy machinery. The core machinery is composed of three major functional groups: (1) Atg9 and its cycling system, which includes Atg9, the Atg1 kinase complex (Atg1 and Atg13), Atg2 and Atg18; (2) the phosphatidylinositol 3-OH kinase (PI(3)K) complex (vacuolar protein sorting (Vps)34, Vps15, Atg6(Vps30) and Atg14); (3) the ubiquitin-like protein (Ubl) system, which includes two Ubl proteins (Atg8 and

Atg12), an activating enzyme (Atg7), two analogues of ubiquitin-conjugating enzymes (Atg10 and Atg3), an Atg8 modifying protease (Atg4), the protein target of Atg12 attachment (Atg5) and Atg16.

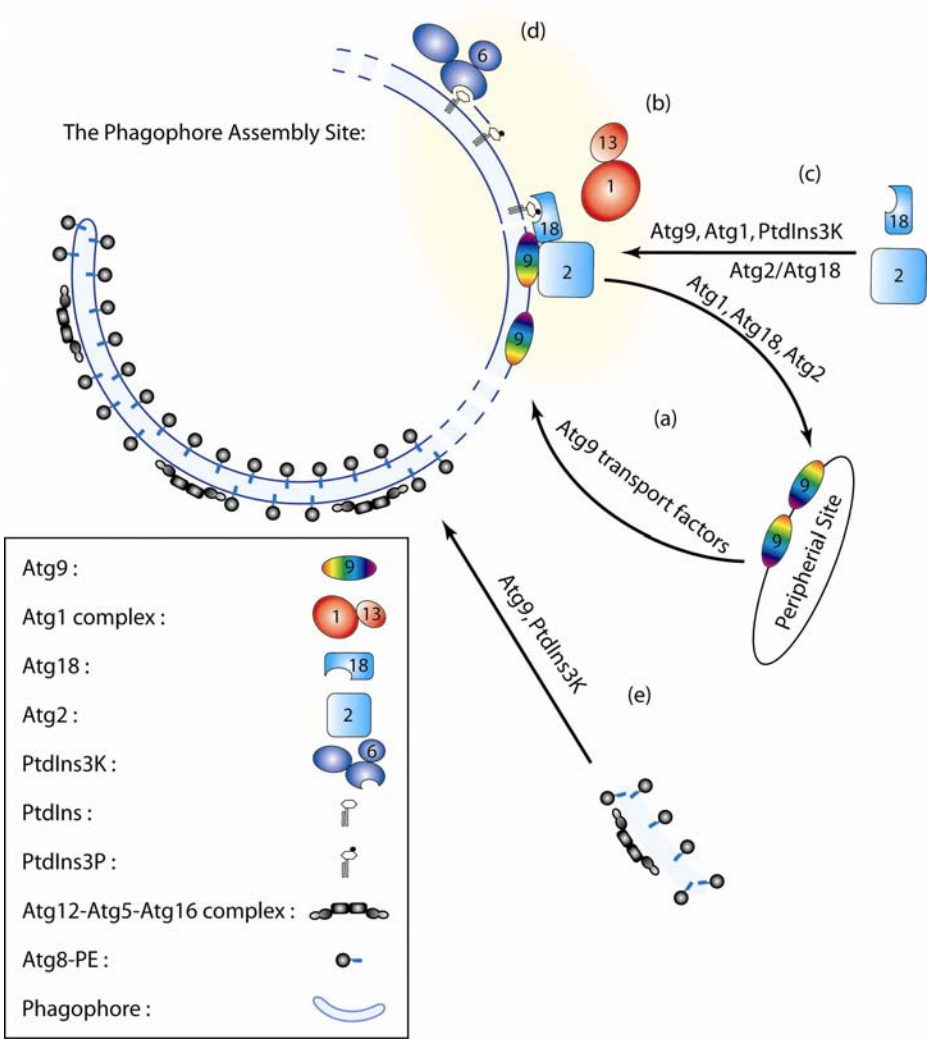

Figure 1.2 The phagophore assembly site (PAS)

The phagophore assembly site (PAS) is the proposed site of autophagosome formation. Depending on the stage of the formation process, the following proteins/protein complexes of the core machinery are present at the PAS. (a) Atg9. Atg9 cycles between the PAS and multiple peripheral sites; Efficient anterograde transport involves Atg9 transport factors, whereas retrograde movement away from the PAS requires the Atg1 kinase complex, Atg18 and Atg2. (b) Atg1 kinase complex. (c) Atg18, Atg2. The PAS localization of these proteins depends on each other, Atg9, Atg1, and the PtdIns3K complex; Atg18 binds PtdIns(3)P. (d) PtdIns3K complex. (e) Atg12—Atg5-Atg16 complex, Atg8—PE; their PAS localization depends on Atg9 and the PtdIns3K complex.

The proposed site for autophagosome formation is the phagophore assembly site (PAS)(Figure 1.2). The PAS can be defined as a hybrid of the forming vesicle (or

phagophore) and the core machinery proteins, the exact configuration of which depends on the stage of autophagosome formation. The concerted actions of the core machinery at the PAS lead to the expansion and metamorphosis of the phagophore into an autophagosome. During this process, most core machinery proteins, except for Atg8, are excluded from the completed vesicle, some being relocated to non-PAS (peripheral) sites.

In *Saccharomyces cerevisiae*, the PAS is a peri-vacuolar site to which most core machinery proteins localize[9, 10]. In mammalian systems, colocalization of core machinery proteins has been observed in many instances, even though a comprehensive study has been lacking[11-14]. In these studies, each cell generally displays multiple sites of Atg protein colocalization, possibly corresponding to multiple PAS. Association between the core machinery proteins and the phagophore has been shown in both yeast and mammalian cells[11, 12, 15, 16].

Atg9 is the only transmembrane protein in the core machinery that is conserved across species[13, 14, 17]. It has six proposed transmembrane domains, with its amino and carboxyl termini exposed in the cytosol[13, 14]. Atg9 is capable of self-interaction and may exist in a complex[18]. A population of Atg9 is localized to the PAS, and, in the absence of Atg9, the Ubl proteins are not recruited to this site[9]. Interestingly, unlike most other Atg proteins whose non-PAS population is diffuse in the cytosol, the non-PAS population of Atg9 is concentrated in punctate structures[17]. The bidirectional movement of Atg9, between the PAS and non-PAS structures, is necessary for autophagosome formation[17, 19, 20]. Potentially, this shuttling could contribute to the delivery of membrane to the PAS[17, 18]. In yeast, some non-PAS Atg9 puncta are found to be adjacent to or at the surface of mitochondria[18]. By contrast, human Atg9 homologues localize to the *trans*-Golgi network and late endosomes[14] but not mitochondria[13]. The efficient delivery of yeast Atg9 to the PAS involves Atg9 transport factors Atg23 and Atg27 (Atg9 transport factors shown in Figure 1.2)[20, 21]. Atg27 is a type I transmembrane protein[20], whereas Atg23 is soluble[22]. Atg9 cannot be detected at the PAS by fluorescence microscopy in the absence of either of the two proteins. However, in contrast to an *atg9Δ* strain, autophagosomes are still produced in an *atg23Δ* or *atg27Δ* strain under starvation conditions, only at a lower rate[20, 22]. One possible explanation for the apparent difference in the requirement for these proteins in autophagosome formation is that Atg23 and Atg27 mainly affect the

efficiency of Atg9 trafficking. Thus, in the absence of Atg23 or Atg27, a small amount of Atg9, below the detection limit of fluorescence microscopy, travels to the PAS and perform its function. Current evidence suggests that Atg23 and Atg27 travel together with Atg9 to the PAS, and that the anterograde transport of all three proteins is largely interdependent[21]; however, the mechanism for releasing the soluble protein Atg23 from the PAS is different from that of the integral membrane proteins Atg9 and Atg27[17, 20]. Finally, the non-PAS population of Atg9 localizes to different sites in yeasts and mammals, indicating that the choice of peripheral storage sites of Atg9 is species dependent[13, 14, 18]. Therefore, the corresponding Atg9 anterograde transport systems could potentially involve unique adaptations in different species even if they still employ similar mechanisms.

The retrieval of Atg9 from the PAS depends on the Atg1 kinase complex, Atg2 and Atg18 (Figure 1.2); the absence of any of these proteins results in Atg9 accumulation at the PAS[17]. Atg1 is a serine/threonine protein kinase[23], and its kinase activity is required for autophagy[23, 24]. Atg13 is a regulatory subunit of the Atg1 complex[23]. Other proteins associated with Atg1 or Atg13 are generally specific for certain subtypes of autophagy[24-26]. The Atg1 kinase complex is proposed to regulate the magnitude of autophagy [23, 24, 26]. Currently, the retrieval of Atg9 from the PAS is the only process that the Atg1 complex is known to regulate[17]. Interestingly, Atg9 is not restricted at the PAS in *atg1Δ* cells carrying an Atg1 mutant with reduced kinase activity[17], but these cells still have an autophagy-defective phenotype. Therefore, Atg1 may have a broader function in autophagy than regulating Atg9 trafficking alone. In human cells, short interfering RNA (siRNA) depletion of *HsAtg1* (*ULK1*), the apparent mammalian homologue of *ATG1*, inhibits the starvation-induced redistribution of HsAtg9 (ATG9L1) from the *trans*-Golgi network to endosomes[14]. Putative homologues of Atg13 are found in other eukaryotes[27], although their involvement in autophagy has not been examined.

Atg18 and Atg2 are two interacting peripheral membrane proteins[28-31]. Their PAS localization depends on each other as well as Atg1, Atg9 and the PI(3)K complex (Figure 1.2)[28-32]. Both Atg2 and Atg18 can interact with Atg9[17, 28]. Atg18 is able to bind to two phosphoinositides, phosphatidylinositol 3-phosphate (PtdIns(3)P) and PtdIns(3,5)P_2[32-34]. The interaction between Atg18 and PtdIns(3)P is required for autophagy[32, 33]. In contrast,

PtdIns(3,5)P_2 recruits Atg18 to the vacuole membrane for retrograde trafficking from the vacuole[32].

The following model has been proposed for the retrieval of Atg9 from the PAS (Figure 1.2; Table 1.1)[17]: in stage 1, Atg9 and the Atg1 complex are separately recruited to the PAS. In stage 2, Atg18 and Atg2 are recruited to the PAS, where they interact with Atg9. In stage 3, Atg9 leaves the PAS. This model is mainly based on analyses of steady-state knockout mutants, as the *in vivo* order in real time has not been observed. Thus, it is not yet clear whether Atg9 cycles only once in a synchronized manner or cycles continuously during the formation of each autophagosome.

Table 1.1 Summary of supporting data for the Atg9 retrieval model

Event	Requirements
Atg9 localizes to the PAS	Atg23*, Atg27* [20]
Atg1 localizes to the PAS	Atg11* or Atg17* [31, 35]
Atg18/Atg2 localizes to the PAS	PtdIns3K, Atg1, Atg9, Atg2/Atg18 [28-32]
Atg2-Atg9 interaction	Not determined
Atg9-Atg18 interaction	Atg1, Atg2 [17]
Atg9 retrieval from the PAS	Atg1, Atg13, Atg2, Atg18 [17]

*These proteins are either not essential for autophagy or specific for certain subtypes of autophagy. See Table 1.2.

Vps34 is a class III PI(3)K. Besides autophagy, it participates in multiple vesicular trafficking pathways involving endosomes and lysosomes[36]. Vps15, a protein kinase required for Vps34 membrane association, interacts with and probably activates Vps34[37, 38]. In *S. cerevisiae,* Vps15 and Vps34, along with Atg6 (Vps30) and Atg14, form the autophagy-specific PI(3)K complex, localizing to the PAS[39, 40]. *S. cerevisiae* also has a second complex containing Vps15, Vps34, Atg6 and Vps38, which participates in the delivery of a subset of vacuolar proteins through the Vps pathway[39, 40]. By contrast, Beclin 1, the mammalian homologue of Atg6[41], is not involved in lysosomal protein delivery or endocytosis; instead it primarily functions in autophagy[42, 43]. So far, mammalian homologues of Atg14 have not been characterized. The PI(3)K complex presumably functions at the PAS by recruiting PtdIns(3)P binding proteins such as

Atg18[32], which participates in Atg9 retrieval[17]. Evidently, additional effectors are present. For example, the localization pattern of Atg9 in *atg14Δ* cells is different from that seen in *atg18Δ* cells[17]. This implies an early role for the PI(3)K in autophagosome formation, although the underlying mechanism and the effectors remain elusive.

The ubiquitin-like protein system includes two Ubl proteins, Atg8 and Atg12[44, 45]. Whereas their primary sequences do not display clear homology to ubiquitin, the crystal structures of Atg8 and Atg12 homologues from mammals and plants, respectively, show that each has a ubiquitin fold at the C terminus[46, 47]. *In vivo*, the C-terminal glycine of Atg8 is attached to phosphatidylethanolamine (PE) and the C-terminal glycine of Atg12 is attached to an internal lysine in Atg5[44, 45, 48, 49]. Before attachment, the C terminus of Atg8 is processed by a cysteine protease, Atg4, to expose the glycine residue[50, 51]. Both modification reactions share a single E1-like activating enzyme, Atg7[44, 45, 52, 53]. The E2-like conjugating enzymes are Atg3 for Atg8[45, 54], and Atg10 for Atg12[55, 56]. Endogenous Atg7 is cytosolic and the attachment of Ubl proteins is normal in strains defective in PAS localization of Ubl proteins, suggesting that the PAS is either not the site of these modification reactions or is not required for them to take place[9, 53].During autophagy, a population of Atg8—PE needs to be released from PE by Atg4[50]. No similar cleavage has been observed for Atg12. Both conjugation systems have been reconstituted *in vitro*[57, 58].

The Atg12-modified Atg5 forms a multimeric complex with Atg16[12, 59, 60]. In this complex, Atg5 interacts with Atg16 on the side opposite to where it covalently attaches to Atg12[61]. The oligomerization of the complex is mediated by the self-interaction of Atg16[12, 59, 60], and the membrane association of the complex is mediated by Atg5[11, 12, 59]. During autophagosome formation, this complex and Atg8—PE decorate the expanding phagophore[11, 12, 15, 16].As the phagophore membrane expands, the Atg12—Atg5-Atg16 complex mainly resides on the outer side, whereas Atg8—PE does not display a preference (Figure 1.2)[11, 12, 15, 16]. Upon completion of autophagosome formation, the Atg12—Atg5-Atg16 complex is released into the cytosol[11, 12]. Meanwhile, a significant amount of Atg8—PE remains in the completed autophagosome during its journey to the lysosome[12, 15, 62]. Following autophagosome-lysosome fusion and lysis of the remaining single-membrane that envelops the cargo, this population of Atg8 is released into the lysosome lumen and degraded.

It is possible that the Ubl proteins have a role in phagophore expansion, although alternative modes of action have been suggested[11, 63]. The PAS localization of the Ubl proteins depends on Atg9 and the autophagy-specific PI(3)K complex, but not on proteins in the Atg9 retrieval system[9, 13]. Additionally, Atg8—PE recruitment to the PAS requires the Atg12—Atg5-Atg16 complex[9, 11, 64]; the level of Atg8—PE *in vivo* is reduced in the absence of Atg12, Atg5 or Atg16[9, 11, 61].

In yeast cells lacking Atg9 or Atg6, the recruitment of Ubl proteins to the PAS is affected, but the level of Atg8—PE is normal, suggesting that the Atg12—Atg5-Atg16 complex resides on Atg8—PE -containing structures before they reach the PAS[9]. Both Atg9 and Atg8—PE are presumably integrated in the membrane and colocalize at the PAS, yet their non-PAS populations display distinct localization patterns: Atg9 is punctate and Atg8 is diffuse. Whether they reside on the same membrane structure at the PAS remains undetermined.

Adaptations of the core machinery

Autophagy can be selective or non-selective (Figure 1.3). During selective autophagy, only pertinent cargoes are sequestered into autophagosomes. The selective autophagosomes, including Cvt vesicles, pexophagosomes and bacteria-containing autophagosomes, have contours that resemble those of the cargoes, contain little bulk cytosol between the cargo and the vesicle inner membrane[28, 63, 65-67]. This suggests that the core machinery is able to incorporate information about the number and shape of the cargoes, and produce vesicles accordingly, or that the vesicles assemble directly around the cargoes, using them as a scaffold. By contrast, during non-selective autophagy, autophagosomes primarily contain bulk cytoplasmic material. Owing to the soluble nature of the cargo, the core machinery conceivably needs additional mechanisms to determine its own workload. Here we discuss modifications and additions (Table 1.2) to the core machinery in subtypes of autophagy in order to understand the mechanism used to achieve different modes of action in selective and non-selective autophagy.

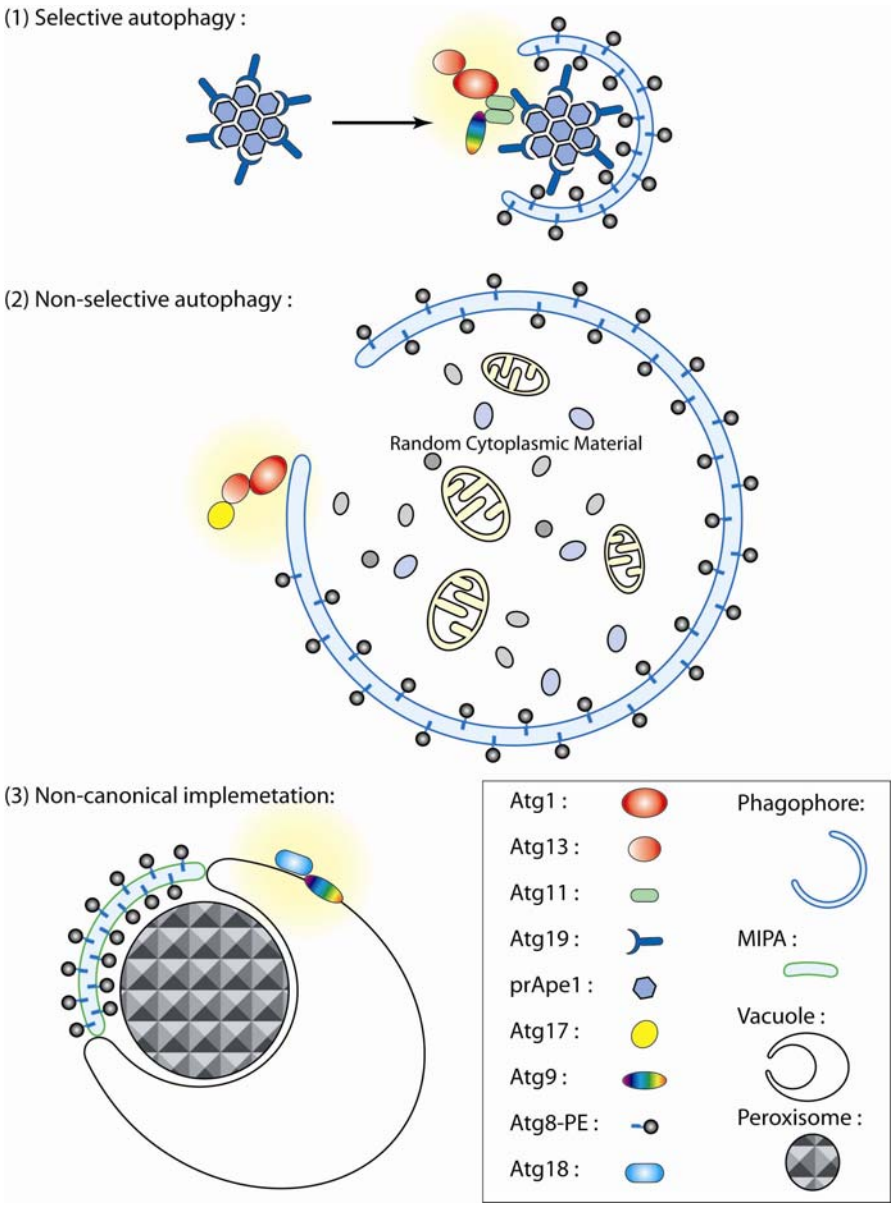

Figure 1.3 Adaptations of the core machinery

(1) Selective autophagy (showing the Cvt pathway as an example). The cargo complex is recognized by the receptor, Atg19. The delivery of the cargo complex to the PAS and the organization of the PAS are mediated by an adapter, Atg11; Atg11 interacts with Atg19, Atg1 and Atg9. Atg19 also interacts with Atg8. (2) Non-selective autophagy. An increase in the magnitude of non-selective autophagy requires regulation of the Atg1 kinase complex that involves Atg17. Meanwhile, the expression and turnover rate of Atg8 is elevated. (3) Non-canonical implementation (showing micropexophagy as an example). Atg9 and Atg18 are involved in forming the vacuole arms. Atg8 is involved in forming the micropexophagic membrane apparatus (MIPA), which is required for the final sequestration.

Table 1.2 Subtype specific *ATG* genes

Gene name	Involvement in autophagy subtypes		
	Cvt pathway	Pexophagy	Non-selective autophagy
ATG11	Yes [25]	Yes [25]	No [25]
ATG17	No [23]	I/M [26]	Yes [23]
ATG19	Yes [68]	No [68]	No [68]
ATG20	Yes [69]	No [69]	No [69]
ATG21	Yes [32]	S/C/D [32, 70]	No [32]
ATG23	Yes [22]	No [22]	I/M [22]
ATG24	Yes [69]	S/C/D [69, 71]	No [69]
ATG25	N/A	Yes [72]	N/A
ATG26	No [73]	S/C/D [73-75]	No [73]
ATG27	I/M [20]	I/M [20]	I/M [20]
ATG28	N/A	Yes [76]	No [76]
ATG29	No [77]	N/A	Yes [77]

Yes: required;
No: not involved;
I/M: knockout strains display intermediate phenotype;
S/C/D: phenotype is species or condition dependent;
N/A: not tested or homologues not present in relevant model systems.

Yeast systems provide two well-characterized examples of selective autophagy. The first and most thoroughly studied example is the Cvt pathway in *S. cerevisiae*, in which at least two precursor hydrolases are delivered to the vacuole to be activated (Figure 1.3)[78, 79]. In the Cvt pathway, the assembly of the PAS is initiated in the presence of the cargo complex[35]. Precursor aminopeptidase I (prApe1), a cargo of the Cvt pathway, oligomerizes into dodecamers, then forms a complex of about 100 nm in diameter in the cytosol[65, 80, 81]. Atg19, the cargo receptor, is then recruited to the prApe1 complex[68]. The delivery of the cargo complex to the PAS and the organization of the PAS are mediated by an adaptor, Atg11[25, 82]. Atg11 interacts with Atg19 and two members of the core machinery, Atg9 and Atg1, in addition to other proteins, possibly regulating the trafficking of Atg9 and the activity of the Atg1 complex[23, 25, 83]. Atg19 also interacts with Atg8, and this interaction might be required for the phagophore to wrap around the

cargo[82]. After completion of autophagosome formation, both the cargo and the receptor are delivered to the vacuole, where the receptor is degraded[68].

The second example of selective autophagy, macropexophagy, involves the degradation of excess peroxisomes, when yeast cells are shifted from media in which peroxisomal enzymes are essential for growth to media where these enzymes are no longer needed. Similar to the Cvt pathway, macropexophagy employs the core autophagy machinery and Atg11, whereas an Atg19-like receptor has not been identified[84].

Examples of selective autophagy are also present in mammals. For instance, selective autophagy plays an active part in innate immune defence against intracellular pathogens. Invading bacteria are generally sequestered into phagosomes *en route* to destruction. Some microbes, such as *Streptococcus pyogenes*, however, have developed the ability to escape into the host cytosol. These intracellular bacteria are then targeted by autophagy, and the sequestering autophagosome membranes closely enwrap the bacteria[85]. Although it is not known how the host autophagy machinery recognizes *Streptococcus*, an interesting clue is provided by *Shigella flexneri*, which has evolved a method to avoid such autophagic attack by masking a surface protein that would otherwise be recognized by the host defense machinery[67]. In this case, the bacterial surface protein VirG, which is involved in motility, is masked by a secreted protein, IscB, a *Shigella* virulence protein. Without IscB, mutant *Shigella* can still escape into the host cytosol. Unlike the wild-type bacteria, however, these mutants are then trapped in autophagosomes. Under these conditions VirG interacts with Atg5; however, the role of this interaction primarily resides on the outside surface of forming autophagosomes.

Another well-known function of autophagy is the removal of aggregate prone proteins[86]. In human cells, a polyubiquitin-binding protein p62 (SQSTM1) links polyubiquitinated aggregates with LC3, a mammalian homologue of Atg8 by binding to both proteins[87]. This can be considered as a reminiscent of the prApe1-complex-Atg19-Atg8 scheme in the Cvt pathway.

Non-selective autophagy has been observed in all eukaryotes analyzed. In general, this process is triggered by starvation, but it also takes place constitutively at a low basal level. Although traditionally considered the *bona fide* form of autophagy, studies in yeast suggest that non-selective autophagy also involves adjustments and additions to the core

machinery (Figure 1.3). This is not unexpected, considering that the induction of non-selective autophagy leads to increases in the size of the sequestering vesicle and in the production rate, compared with the Cvt pathway[80, 88]. Therefore, an acceleration of the membrane supply is also expected. Several of the changes that take place during non-selective autophagy in response to starvation center on the Atg1 kinase complex. First, the kinase activity of Atg1 is increased (on the basis of *in vitro* assays)[23, 24]. This is accompanied by dephosphorylation of Atg13, which results in stronger affinity for Atg1 and Atg17, the latter being a protein uniquely required for non-selective autophagy[23, 24, 26]. The absence of Atg17 causes a severe reduction in both Atg1 activity and the magnitude of non-selective autophagy[24, 26]. Additionally, the expression level and turnover rate of Atg8 is elevated, a phenomenon observed in other eukaryotes as well[15, 62, 89]. It is noteworthy that starvation enhances lysosome biogenesis[90, 91], which might coordinate with autophagy induction; however, this should not be interpreted as direct evidence of autophagy.

The aforementioned selective and nonselective types of autophagy all follow the canonical scheme with formation of autophagosomes in the cytosol and subsequent fusion with a lysosome. However, the core machinery can also function in a non-canonical form. In *Pichia pastoris*, depending on the physiological conditions, peroxisomes are degraded either through macropexophagy or micropexophagy[84]. In micropexophagy, peroxisomes are sequestered mainly by arm-like extensions or septations of the vacuole, which are then sealed through a process that involves a small membrane patch, the micropexophagic membrane apparatus (MIPA)(Figure 1.3)[92]. Micropexophagy uses the same core machinery proteins as macropexophagy, although in a different organizational pattern, despite the fact that the two pathways are morphologically distinct (Figure 1.3). For example, Atg9 and Atg18 localize to the vacuole membrane and participate in forming the extending vacuole arms during micropexophagy[28, 93]. In this case, the role of the Ubl system might be restricted to the formation of the MIPA, which contains Atg8[92]. An analogy may be that of a plastic wrap, which can be used to cover different items in various configurations, but in all cases carries out a similar function.

Homologues of proteins of the core machinery have been identified from yeasts to mammals, and most of them participate in autophagy. Conversely, proteins required specifically in certain subtypes of autophagy, such as Atg17 in starvation-induced non-selective autophagy and Atg11 in selective autophagy, are not conserved. It is tempting to speculate that during evolution, the core machinery of autophagosome formation has been preserved; but, this core has also been modified and supplemented with specific factors in different species for adaptation to their unique environmental niche.

Currently, our knowledge of the organization and functions of the core machinery is still quite limited, in part because very few of the Atg proteins have clear functional motifs. accordingly, continued efforts are needed to elucidate the most complex part of autophagy, the formation of the autophagosome. Furthermore, there are differences between autophagy that is induced by starvation and the process that is initiated in response to pathogen invasion or other pathological conditions. Thus, the unique adaptations that allow autophagy to meet various physiological conditions should not be overlooked.

References

1. Yorimitsu T, Klionsky DJ. Autophagy: molecular machinery for self-eating. Cell Death Differ. 2005; 12:1542-52.

2. Levine B, Klionsky DJ. Development by self-digestion: molecular mechanisms and biological functions of autophagy. Dev. Cell 2004; 6:463-77.

3. Shintani T, Klionsky DJ. Autophagy in health and disease: a double-edged sword. Science 2004; 306:990-5.

4. Munz C. Autophagy and antigen presentation. Cell. Microbiol. 2006; 8:891-8.

5. Kunz JB, Schwarz H, Mayer A. Determination of four sequential stages during microautophagy *in vitro*. J. Biol. Chem. 2004; 279:9987-96.

6. Majeski AE, Dice JF. Mechanisms of chaperone-mediated autophagy. Int J Biochem Cell Biol. 2004; 36:2435-44.

7. Kvam E, Goldfarb DS. Nucleus-vacuole junctions and piecemeal microautophagy of the nucleus in *S. cerevisiae*. Autophagy 2007; 3:85-92.

8. Klionsky DJ, Cregg JM, Dunn WA, Jr., Emr SD, Sakai Y, Sandoval IV, Sibirny A, Subramani S, Thumm M, Veenhuis M, Ohsumi Y. A unified nomenclature for yeast autophagy-related genes. Dev. Cell 2003; 5:539-45.

9. Suzuki K, Kirisako T, Kamada Y, Mizushima N, Noda T, Ohsumi Y. The pre-autophagosomal structure organized by concerted functions of *APG* genes is essential for autophagosome formation. EMBO J. 2001; 20:5971-81.

10. Kim J, Huang W-P, Stromhaug PE, Klionsky DJ. Convergence of multiple autophagy and cytoplasm to vacuole targeting components to a perivacuolar membrane compartment prior to *de novo* vesicle formation. J. Biol. Chem. 2002; 277:763-73.

11. Mizushima N, Yamamoto A, Hatano M, Kobayashi Y, Kabeya Y, Suzuki K, Tokuhisa T, Ohsumi Y, Yoshimori T. Dissection of autophagosome formation using Apg5-deficient mouse embryonic stem cells. J. Cell Biol. 2001; 152:657-68.

12. Mizushima N, Kuma A, Kobayashi Y, Yamamoto A, Matsubae M, Takao T, Natsume T, Ohsumi Y, Yoshimori T. Mouse Apg16L, a novel WD-repeat protein, targets to the autophagic isolation membrane with the Apg12-Apg5 conjugate. J. Cell Sci. 2003; 116:1679-88.

13. Yamada T, Carson AR, Caniggia I, Umebayashi K, Yoshimori T, Nakabayashi K, Scherer SW. Endothelial nitric-oxide synthase antisense (NOS3AS) gene encodes an autophagy-related protein (APG9-like2) highly expressed in trophoblast. J. Biol. Chem. 2005; 280:18283-90.

14. Young ARJ, Chan EYW, Hu XW, Köchl R, Crawshaw SG, High S, Hailey DW, Lippincott-Schwartz J, Tooze SA. Starvation and ULK1-dependent cycling of mammalian Atg9 between the TGN and endosomes. J. Cell Sci. 2006; 119:3888-900.

15. Kirisako T, Baba M, Ishihara N, Miyazawa K, Ohsumi M, Yoshimori T, Noda T, Ohsumi Y. Formation process of autophagosome is traced with Apg8/Aut7p in yeast. J. Cell Biol. 1999; 147:435-46.

16. Kabeya Y, Mizushima N, Ueno T, Yamamoto A, Kirisako T, Noda T, Kominami E, Ohsumi Y, Yoshimori T. LC3, a mammalian homologue of yeast Apg8p, is localized in autophagosome membranes after processing. EMBO J. 2000; 19:5720-8.

17. Reggiori F, Tucker KA, Stromhaug PE, Klionsky DJ. The Atg1-Atg13 complex regulates Atg9 and Atg23 retrieval transport from the pre-autophagosomal structure. Dev. Cell 2004; 6:79-90.

18. Reggiori F, Shintani T, Nair U, Klionsky DJ. Atg9 cycles between mitochondria and the pre-autophagosomal structure in yeasts. Autophagy 2005; 1:101-9.

19. Reggiori F, Klionsky DJ. Atg9 sorting from mitochondria is impaired in early secretion and VFT-complex mutants in *Saccharomyces cerevisiae*. J. Cell Sci. 2006; 119:2903-11.

20. Yen W-L, Legakis JE, Nair U, Klionsky DJ. Atg27 is required for autophagy-dependent cycling of Atg9. Mol. Biol. Cell. 2006.

21. Legakis JE, Yen W-L, Klionsky DJ. A cycling protein complex required for selective autophagy. Autophagy 2007; 3:422-32.

22. Tucker KA, Reggiori F, Dunn WA, Jr., Klionsky DJ. Atg23 is essential for the cytoplasm to vacuole targeting pathway and efficient autophagy but not pexophagy. J. Biol. Chem. 2003; 278:48445-52.

23. Kamada Y, Funakoshi T, Shintani T, Nagano K, Ohsumi M, Ohsumi Y. Tor-mediated induction of autophagy via an Apg1 protein kinase complex. J. Cell Biol. 2000; 150:1507-13.

24. Kabeya Y, Kamada Y, Baba M, Takikawa H, Sasaki M, Ohsumi Y. Atg17 functions in cooperation with Atg1 and Atg13 in yeast autophagy. Mol. Biol. Cell. 2005; 16:2544-53.

25. Kim J, Kamada Y, Stromhaug PE, Guan J, Hefner-Gravink A, Baba M, Scott SV, Ohsumi Y, Dunn WA, Jr., Klionsky DJ. Cvt9/Gsa9 functions in sequestering selective cytosolic cargo destined for the vacuole. J. Cell Biol. 2001; 153:381-96.

26. Cheong H, Yorimitsu T, Reggiori F, Legakis JE, Wang C-W, Klionsky DJ. Atg17 regulates the magnitude of the autophagic response. Mol. Biol. Cell. 2005; 16:3438-53.

27. Meijer WH, van der Klei IJ, Veenhuis M, Kiel JAKW. *ATG* genes involved in non-selective autophagy are conserved from yeast to man, but the selective Cvt and pexophagy pathways also require organism-specific genes. Autophagy 2007; 3:106-16.

28. Guan J, Stromhaug PE, George MD, Habibzadegah-Tari P, Bevan A, Dunn WA, Jr., Klionsky DJ. Cvt18/Gsa12 is required for cytoplasm-to-vacuole transport, pexophagy, and autophagy in *Saccharomyces cerevisiae* and *Pichia pastoris*. Mol. Biol. Cell. 2001; 12:3821-38.

29. Shintani T, Suzuki K, Kamada Y, Noda T, Ohsumi Y. Apg2p functions in autophagosome formation on the perivacuolar structure. J. Biol. Chem. 2001; 276:30452-60.

30. Wang C-W, Kim J, Huang W-P, Abeliovich H, Stromhaug PE, Dunn WA, Jr., Klionsky DJ. Apg2 is a novel protein required for the cytoplasm to vacuole targeting, autophagy, and pexophagy pathways. J. Biol. Chem. 2001; 276:30442-51.

31. Suzuki K, Kubota Y, Sekito T, Ohsumi Y. Hierarchy of Atg proteins in pre-autophagosomal structure organization. Genes Cells 2007; 12:209-18.

32. Stromhaug PE, Reggiori F, Guan J, Wang C-W, Klionsky DJ. Atg21 is a phosphoinositide binding protein required for efficient lipidation and localization of Atg8 during uptake of aminopeptidase I by selective autophagy. Mol. Biol. Cell. 2004; 15:3553-66.

33. Dove SK, Piper RC, McEwen RK, Yu JW, King MC, Hughes DC, Thuring J, Holmes AB, Cooke FT, Michell RH, Parker PJ, Lemmon MA. Svp1p defines a family of phosphatidylinositol 3,5-bisphosphate effectors. EMBO J. 2004; 23:1922-33.

34. Proikas-Cezanne T, Waddell S, Gaugel A, Frickey T, Lupas A, Nordheim A. WIPI-1alpha (WIPI49), a member of the novel 7-bladed WIPI protein family, is aberrantly expressed in human cancer and is linked to starvation-induced autophagy. Oncogene 2004; 23:9314-25.

35. Shintani T, Klionsky DJ. Cargo proteins facilitate the formation of transport vesicles in the cytoplasm to vacuole targeting pathway. J. Biol. Chem. 2004; 279:29889-94.

36. Lindmo K, Stenmark H. Regulation of membrane traffic by phosphoinositide 3-kinases. J. Cell Sci. 2006; 119:605-14.

37. Stack JH, Herman PK, Schu PV, Emr SD. A membrane-associated complex containing the Vps15 protein kinase and the Vps34 PI 3-kinase is essential for protein sorting to the yeast lysosome-like vacuole. EMBO J. 1993; 12:2195-204.

38. Panaretou C, Domin J, Cockcroft S, Waterfield MD. Characterization of p150, an adaptor protein for the human phosphatidylinositol (PtdIns) 3-kinase. Substrate presentation by phosphatidylinositol transfer protein to the p150.Ptdins 3-kinase complex. J. Biol. Chem. 1997; 272:2477-85.

39. Kihara A, Noda T, Ishihara N, Ohsumi Y. Two distinct Vps34 phosphatidylinositol 3-kinase complexes function in autophagy and carboxypeptidase Y sorting in *Saccharomyces cerevisiae*. J. Cell Biol. 2001; 152:519-30.

40. Obara K, Sekito T, Ohsumi Y. Assortment of phosphatidylinositol 3-kinase complexes--Atg14p directs association of complex I to the pre-autophagosomal structure in *Saccharomyces cerevisiae*. Mol. Biol. Cell. 2006; 17:1527-39.

41. Liang XH, Jackson S, Seaman M, Brown K, Kempkes B, Hibshoosh H, Levine B. Induction of autophagy and inhibition of tumorigenesis by *beclin 1*. Nature 1999; 402:672-6.

42. Furuya N, Yu J, Byfield M, Pattingre S, Levine B. The evolutionarily conserved domain of Beclin 1 is required for Vps34 binding, autophagy and tumor suppressor function. Autophagy 2005; 1:46-52.

43. Zeng X, Overmeyer JH, Maltese WA. Functional specificity of the mammalian Beclin-Vps34 PI 3-kinase complex in macroautophagy versus endocytosis and lysosomal enzyme trafficking. J. Cell Sci. 2006; 119:259-70.

44. Mizushima N, Noda T, Yoshimori T, Tanaka Y, Ishii T, George MD, Klionsky DJ, Ohsumi M, Ohsumi Y. A protein conjugation system essential for autophagy. Nature 1998; 395:395-8.

45. Ichimura Y, Kirisako T, Takao T, Satomi Y, Shimonishi Y, Ishihara N, Mizushima N, Tanida I, Kominami E, Ohsumi M, Noda T, Ohsumi Y. A ubiquitin-like system mediates protein lipidation. Nature 2000; 408:488-92.

46. Paz Y, Elazar Z, Fass D. Structure of GATE-16, membrane transport modulator and mammalian ortholog of autophagocytosis factor Aut7p. J. Biol. Chem. 2000; 275:25445-50.

47. Suzuki NN, Yoshimoto K, Fujioka Y, Ohsumi Y, Inagaki F. The crystal structure of plant ATG12 and its biological implication in autophagy. Autophagy 2005; 1:119-26.

48. Mizushima N, Sugita H, Yoshimori T, Ohsumi Y. A new protein conjugation system in human. The counterpart of the yeast Apg12p conjugation system essential for autophagy. J. Biol. Chem. 1998; 273:33889-92.

49. Sou YS, Tanida I, Komatsu M, Ueno T, Kominami E. Phosphatidylserine in addition to phosphatidylethanolamine is an in vitro target of the mammalian Atg8 modifiers, LC3, GABARAP, and GATE-16. J. Biol. Chem. 2006; 281:3017-24.

50. Kirisako T, Ichimura Y, Okada H, Kabeya Y, Mizushima N, Yoshimori T, Ohsumi M, Takao T, Noda T, Ohsumi Y. The reversible modification regulates the membrane-binding state of Apg8/Aut7 essential for autophagy and the cytoplasm to vacuole targeting pathway. J. Cell Biol. 2000; 151:263-76.

51. Hemelaar J, Lelyveld VS, Kessler BM, Ploegh HL. A single protease, Apg4B, is specific for the autophagy-related ubiquitin-like proteins GATE-16, MAP1-LC3, GABARAP, and Apg8L. J. Biol. Chem. 2003; 278:51841-50.

52. Tanida I, Tanida-Miyake E, Ueno T, Kominami E. The human homolog of *Saccharomyces cerevisiae* Apg7p is a Protein-activating enzyme for multiple substrates including human Apg12p, GATE-16, GABARAP, and MAP-LC3. J. Biol. Chem. 2001; 276:1701-6.

53. Tanida I, Mizushima N, Kiyooka M, Ohsumi M, Ueno T, Ohsumi Y, Kominami E. Apg7p/Cvt2p: A novel protein-activating enzyme essential for autophagy. Mol. Biol. Cell. 1999; 10:1367-79.

54. Tanida I, Tanida-Miyake E, Komatsu M, Ueno T, Kominami E. Human Apg3p/Aut1p homologue is an authentic E2 enzyme for multiple substrates, GATE-16, GABARAP, and MAP-LC3, and facilitates the conjugation of hApg12p to hApg5p. J. Biol. Chem. 2002; 277:13739-44.

55. Shintani T, Mizushima N, Ogawa Y, Matsuura A, Noda T, Ohsumi Y. Apg10p, a novel protein-conjugating enzyme essential for autophagy in yeast. EMBO J. 1999; 18:5234-41.

56. Nemoto T, Tanida I, Tanida-Miyake E, Minematsu-Ikeguchi N, Yokota M, Ohsumi M, Ueno T, Kominami E. The mouse *APG10* homologue, an E2-like enzyme for Apg12p conjugation, facilitates MAP-LC3 modification. J. Biol. Chem. 2003; 278:39517-26.

57. Ichimura Y, Imamura Y, Emoto K, Umeda M, Noda T, Ohsumi Y. *In vivo* and *in vitro* reconstitution of Atg8 conjugation essential for autophagy. J. Biol. Chem. 2004; 279:40584-92.

58. Shao Y, Gao Z, Feldman T, Jiang X. Stimulation of ATG12-ATG5 conjugation by ribonucleic acid. Autophagy 2007; 3:10-6.

59. Mizushima N, Noda T, Ohsumi Y. Apg16p is required for the function of the Apg12p-Apg5p conjugate in the yeast autophagy pathway. EMBO J. 1999; 18:3888-96.

60. Kuma A, Mizushima N, Ishihara N, Ohsumi Y. Formation of the approximately 350-kDa Apg12-Apg5·Apg16 multimeric complex, mediated by Apg16 oligomerization, is essential for autophagy in yeast. J. Biol. Chem. 2002; 277:18619-25.

61. Matsushita M, Suzuki NN, Obara K, Fujioka Y, Ohsumi Y, Inagaki F. Structure of Atg5·Atg16, a complex essential for autophagy. J Biol Chem 2007; 282:6763-72.

62. Huang WP, Scott SV, Kim J, Klionsky DJ. The itinerary of a vesicle component, Aut7p/Cvt5p, terminates in the yeast vacuole via the autophagy/Cvt pathways. J. Biol. Chem. 2000; 275:5845-51.

63. Monastyrska I, van der Heide M, Krikken AM, Kiel JA, van der Klei IJ, Veenhuis M. Atg8 is essential for macropexophagy in Hansenula polymorpha. Traffic 2005; 6:66-74.

64. Kim J, Huang W-P, Klionsky DJ. Membrane recruitment of Aut7p in the autophagy and cytoplasm to vacuole targeting pathways requires Aut1p, Aut2p, and the autophagy conjugation complex. J. Cell Biol. 2001; 152:51-64.

65. Scott SV, Baba M, Ohsumi Y, Klionsky DJ. Aminopeptidase I is targeted to the vacuole by a nonclassical vesicular mechanism. J. Cell Biol. 1997; 138:37-44.

66. Sakai Y, Koller A, Rangell LK, Keller GA, Subramani S. Peroxisome degradation by microautophagy in *Pichia pastoris*: identification of specific steps and morphological intermediates. J. Cell Biol. 1998; 141:625-36.

67. Ogawa M, Yoshimori T, Suzuki T, Sagara H, Mizushima N, Sasakawa C. Escape of intracellular *Shigella* from autophagy. Science 2005; 307:727-31.

68. Scott SV, Guan J, Hutchins MU, Kim J, Klionsky DJ. Cvt19 is a receptor for the cytoplasm-to-vacuole targeting pathway.Mol. Cell 2001; 7:1131-41.

69. Nice DC, Sato TK, Stromhaug PE, Emr SD, Klionsky DJ. Cooperative binding of the cytoplasm to vacuole targeting pathway proteins, Cvt13 and Cvt20, to

phosphatidylinositol 3-phosphate at the pre-autophagosomal structure is required for selective autophagy. J. Biol. Chem. 2002; 277:30198-207.

70. Leao-Helder AN, Krikken AM, Gellissen G, van der Klei IJ, Veenhuis M, Kiel JA. Atg21p is essential for macropexophagy and microautophagy in the yeast *Hansenula polymorpha*. FEBS Lett. 2004; 577:491-5.

71. Ano Y, Hattori T, Oku M, Mukaiyama H, Baba M, Ohsumi Y, Kato N, Sakai Y. A sorting nexin PpAtg24 regulates vacuolar membrane dynamics during pexophagy via binding to phosphatidylinositol-3-phosphate. Mol. Biol. Cell. 2005; 16:446-57.

72. Monastyrska I, Kiel JA, Krikken AM, Komduur JA, Veenhuis M, van der Klei IJ. The *Hansenula polymorpha ATG25* gene encodes a novel coiled-coil protein that is required for macropexophagy. Autophagy 2005; 1:92-100.

73. Cao Y, Klionsky DJ. Atg26 is not involved in autophagy-related pathways in *Saccharomyces cerevisiae*. Autophagy 2007; 3:17-20.

74. Oku M, Warnecke D, Noda T, Muller F, Heinz E, Mukaiyama H, Kato N, Sakai Y. Peroxisome degradation requires catalytically active sterol glucosyltransferase with a GRAM domain. EMBO J. 2003; 22:3231-41.

75. Nazarko TY, Polupanov AS, Manjithaya RR, Subramani S, Sibirny AA. The requirement of sterol glucoside for pexophagy in yeast is dependent on the species and nature of peroxisome inducers. Mol. Biol. Cell. 2007; 18:106-18.

76. Stasyk OV, Stasyk OG, Mathewson RD, Farre JC, Nazarko VY, Krasovska OS, Subramani S, Cregg JM, Sibirny AA. Atg28, a novel coiled-coil protein involved in autophagic degradation of peroxisomes in the methylotrophic yeast *Pichia pastoris*. Autophagy 2006; 2:30-8.

77. Kawamata T, Kamada Y, Suzuki K, Kuboshima N, Akimatsu H, Ota S, Ohsumi M, Ohsumi Y. Characterization of a novel autophagy-specific gene, *ATG29*. Biochem. Biophys. Res. Commun. 2005; 338:1884-9.

78. Klionsky DJ, Cueva R, Yaver DS. Aminopeptidase I of *Saccharomyces cerevisiae* is localized to the vacuole independent of the secretory pathway. J. Cell Biol. 1992; 119:287-99.

79. Scott SV, Hefner-Gravink A, Morano KA, Noda T, Ohsumi Y, Klionsky DJ. Cytoplasm-to-vacuole targeting and autophagy employ the same machinery to deliver proteins to the yeast vacuole. Proc. Natl. Acad. Sci. USA 1996; 93:12304-8.

80. Baba M, Osumi M, Scott SV, Klionsky DJ, Ohsumi Y. Two distinct pathways for targeting proteins from the cytoplasm to the vacuole/lysosome. J. Cell Biol. 1997; 139:1687-95.

81. Kim J, Scott SV, Oda MN, Klionsky DJ. Transport of a large oligomeric protein by the cytoplasm to vacuole protein targeting pathway. J. Cell Biol. 1997; 137:609-18.

82. Shintani T, Huang W-P, Stromhaug PE, Klionsky DJ. Mechanism of cargo selection in the cytoplasm to vacuole targeting pathway. Dev. Cell 2002; 3:825-37.

83. He C, Song H, Yorimitsu T, Monastyrska I, Yen W-L, Legakis JE, Klionsky DJ. Recruitment of Atg9 to the preautophagosomal structure by Atg11 is essential for selective autophagy in budding yeast. J. Cell Biol. 2006; 175:925-35.

84. Dunn WA, Jr., Cregg JM, Kiel JA, van der Klei IJ, Oku M, Sakai Y, Sibirny AA, Stasyk OV, Veenhuis M. Pexophagy: the selective autophagy of peroxisomes. Autophagy 2005; 1:75-83.

85. Nakagawa I, Amano A, Mizushima N, Yamamoto A, Yamaguchi H, Kamimoto T, Nara A, Funao J, Nakata M, Tsuda K, Hamada S, Yoshimori T. Autophagy defends cells against invading group A *Streptococcus*. Science 2004; 306:1037-40.

86. Rubinsztein DC, DiFiglia M, Heintz N, Nixon RA, Qin ZH, Ravikumar B, Stefanis L, Tolkovsky A. Autophagy and its possible roles in nervous system diseases, damage and repair. Autophagy 2005; 1:11-22.

87. Bjorkoy G, Lamark T, Brech A, Outzen H, Perander M, Overvatn A, Stenmark H, Johansen T. p62/SQSTM1 forms protein aggregates degraded by autophagy and has a protective effect on huntingtin-induced cell death. J. Cell Biol. 2005; 171:603-14.

88. Takeshige K, Baba M, Tsuboi S, Noda T, Ohsumi Y. Autophagy in yeast demonstrated with proteinase-deficient mutants and conditions for its induction. J. Cell Biol. 1992; 119:301-11.

89. Tanida I, Minematsu-Ikeguchi N, Ueno T, Kominami E. Lysosomal turnover, but not a cellular level, of endogenous LC3 is a marker for autophagy. Autophagy 2005; 1:84-91.

90. Hamasaki M, Noda T, Ohsumi Y. The early secretory pathway contributes to autophagy in yeast. Cell Struct. Funct. 2003; 28:49-54.

91. Bampton ET, Goemans CG, Niranjan D, Mizushima N, Tolkovsky AM. The dynamics of autophagy visualized in live cells: from autophagosome formation to fusion with endo/lysosomes. Autophagy 2005; 1:23-36.

92. Mukaiyama H, Baba M, Osumi M, Aoyagi S, Kato N, Ohsumi Y, Sakai Y. Modification of a ubiquitin-like protein Paz2 conducted micropexophagy through formation of a novel membrane structure. Mol. Biol. Cell. 2004; 15:58-70.

93. Chang T, Schroder LA, Thomson JM, Klocman AS, Tomasini AJ, Stromhaug PE, Dunn WA, Jr. *PpATG9* encodes a novel membrane protein that traffics to vacuolar membranes, which sequester peroxisomes during pexophagy in *Pichia pastoris*. Mol. Biol. Cell. 2005; 16:4941-53.

Chapter 2
Atg8 Controls Phagophore Expansion during Autophagosome Formation

Abstract

Autophagy is a potent intracellular degradation process with pivotal roles in health and disease. Atg8, a lipid conjugated ubiquitin-like protein, is required for the formation of autophagosomes, double-membrane vesicles responsible for the delivery of cytoplasmic material to lysosomes. How and when Atg8 functions in this process, however, is not clear. Here we show that Atg8 controls the expansion of the autophagosome precursor, the phagophore, and give the first real-time, observation-based temporal dissection of the autophagosome formation process. We demonstrate that the amount of Atg8 determines the size of autophagosomes. During autophagosome biogenesis, Atg8 forms an expanding structure and later dissociates from the site of vesicle formation. Based on the dynamics of Atg8, we present a multi-stage model of autophagosome formation. This model provides a foundation for future analyses of the functions and dynamics of known autophagy-related proteins and for screening new genes.

Introduction

Eukaryotic cells employ macroautophagy, hereafter referred to as autophagy, to eliminate objects ranging from soluble proteins to entire organelles [1]. In multi-cellular organisms, autophagy has important roles in development, immune defense, programmed cell death, tumor suppression, and the prevention of neuronal degeneration [2-5]. In this pathway, cytoplasmic materials are sequestered into an expanding membrane sac, the phagophore, which subsequently matures into a double-membrane vesicle, the autophagosome. The site of autophagosome formation is termed the phagophore assembly site (PAS) [6, 7]. Each autophagosome eventually fuses with a lysosome, resulting in the degradation of the inner membrane and the cargos. The formation of autophagosomes depends on the concerted actions of core autophagy machinery proteins [1, 8].

Among the core machinery proteins is Atg8, a ubiquitin-like protein (UBL) [9, 10]. Newly synthesized Atg8 is processed by a cysteine protease, Atg4, to expose its carboxyl terminal glycine residue [11-13]. It is then conjugated to phosphatidylethanolamine (PE) by the E1-like activating enzyme Atg7 and the E2-like conjugating enzyme Atg3 [9, 14-16]. Conjugated Atg8 can also be deconjugated by Atg4 [11]. A multimeric protein complex formed by Atg12, Atg5, and Atg16 facilitates the conjugation of Atg8, possibly by serving as an E3-like enzyme [6, 17]. The formation of this complex itself also involves a conjugation reaction, in which the UBL Atg12 is attached to Atg5 by Atg7 and the E2-like enzyme Atg10 [18-21].

During autophagy, Atg8 localizes to the PAS. In addition to PE conjugation and the Atg12–Atg5-Atg16 complex, its proper localization requires Atg9, a transmembrane protein suggested as a membrane carrier, and the autophagy-specific phosphatidylinositol 3-kinase (PI3K) complex [6, 11, 12, 22-25]. The PAS population of Atg8 is presumably associated with the phagophore [26-28]. When the phagophore matures into an autophagosome, some Atg8 is trapped inside and eventually degraded [26, 27, 29, 30]. The absence of Atg8 does not apparently affect the function of any other core machinery

proteins [6, 25]. Although Atg8 has been widely used as a marker for recognition of autophagosomes [31], its exact *in vivo* function is still not clear.

In the yeast *Saccharomyces cerevisiae*, the core machinery proteins are shared between starvation-induced autophagy and a second autophagy-like process, the cytoplasm to vacuole targeting (Cvt) pathway, which transports hydrolase precursors from the cytosol to the vacuole (a lysosome analogue) under nutrient rich conditions [1, 32]. Among these proteins, only Atg8 has a significantly elevated protein level when autophagy is induced by starvation, making it a natural candidate for an autophagy regulator [26, 29]. Here we investigated the role of Atg8 through morphological and functional analyses.

Results

Atg8 Regulates the Level of Autophagy

To explore the possible role of Atg8 in autophagy regulation, we generated strains (A8-1, A8-2, and A8-3) that express different levels of Atg8 (Figure 2.1A; Materials and methods). Under nitrogen starvation conditions, the amounts of both conjugated and unconjugated Atg8 in these strains were lower than those of the wild type (Figure 2.1A). We then quantified the levels of autophagy in these strains using the Pho8Δ60 assay [33]. This assay is based on the autophagy-dependent delivery of a non-specific cytosolic marker, the modified phosphatase precursor Pho8Δ60, from the cytosol to the vacuole, where it gets activated. The resulting alkaline phosphatase (ALP) activity thus indicates the total internal volume of autophagosomes. In wild-type cells, nitrogen starvation led to a sharp increase of Pho8Δ60-dependent ALP activity (Figure 2.1B). In contrast, the *atg8*Δ strain showed a negligible increase. Strains A8-1, A8-2 and A8-3 showed intermediate increases, which correlated with their Atg8 protein levels. Importantly, these results were not caused by long-term low-level expression of Atg8 (i.e., a chronic defect), because in nutrient-rich media the levels of Atg8 in strains A8-1, A8-2 and A8-3 were similar to that of the wild-type strain (Figure 2.1A). This level of Atg8 was sufficient for

the maturation of the Cvt pathway cargo, precursor aminopeptidase I (prApe1) (Figure 2.1C). Thus, the levels of Atg8 directly determine levels of autophagy in the corresponding strains.

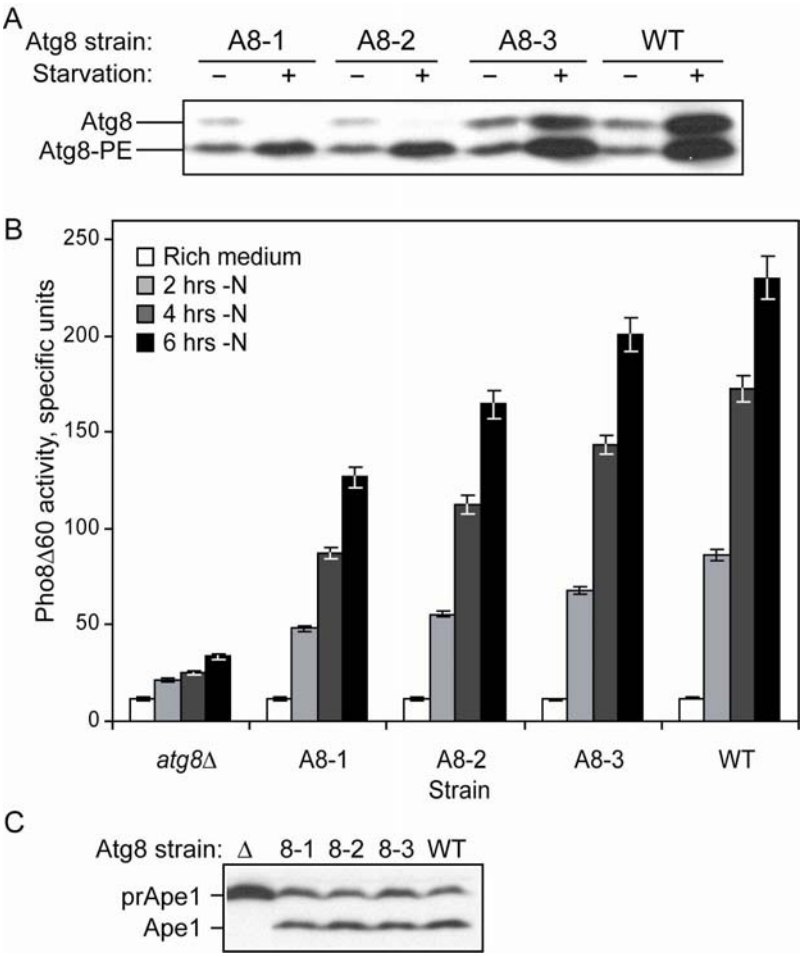

Figure 2.1 Atg8 regulates the level of autophagy

(A) Strains A8-1, A8-2, and A8-3 showed intermediate Atg8 protein levels. Yeast cells were grown in rich medium to mid-log phase, then starved in nitrogen starvation medium for 4 h. Protein extracts were analyzed by immunoblotting with anti-Atg8 antiserum. Atg8—PE, Atg8 conjugated to phosphatidylethanolamine. (B) Atg8 limits the level of autophagy. Yeast cells were grown in rich medium to mid-log phase, and then shifted to nitrogen starvation medium. At the indicated time points, samples were collected and tested by the Pho8Δ60 assay. Specific units, specific activity units (μmoles phosphate/mg/min) normalized to protein concentration. Error bar, S.E.M. (standard error of mean) from six independent repeats. (C) The Cvt pathway is normal in strains A8-1, A8-2, and A8-3. Yeast cells grown in rich medium were collected at mid-log phase; protein extracts were analyzed by immunoblotting with anti-Ape1 antiserum. The locations of precursor and mature Ape1 are indicated.

Atg8 Controls the Size of the Autophagosome

Normal recruitment of Atg8 to the PAS requires Atg9 [6, 25]. It has been shown that slowing the anterograde trafficking of Atg9 leads to retarded autophagosome formation without affecting autophagosome size, possibly by reducing the membrane supply [34]. To explore whether Atg8 functions in a similar manner, we analyzed the effect of lower Atg8 expression by transmission electron microscopy (EM).

Strains expressing variable levels of Atg8 were deleted for the *PEP4* locus. Pep4-dependent vacuolar hydrolase activity is required for degradation of the inner vesicles of autophagosomes (termed autophagic bodies) in the vacuole. Hence, the absence of *PEP4* allows the preservation of autophagic bodies. After 4 hours of starvation, no autophagic bodies were observed in *atg8*Δ *pep4*Δ strains (Figure 2.2A), showing that *atg8*Δ cells are unable to produce autophagosomes; in A8-1, A8-2, A8-3 and wild-type strains deleted for *PEP4*, autophagic bodies abounded in the vacuoles (Figure 2.2A). Lower levels of Atg8 led to significant reductions in sizes of autophagosomes. The average cross sectional radii of autophagic bodies in the A8-1, A8-2, and A8-3 *pep4*Δ strains were 115±2, 125±2, and 148±2, respectively, whereas that of the wild-type *pep4Δ* strain was 162±2 nm (Mean ± S.E.M., n>200) (Figure 2.2B). In contrast, the numbers of autophagic bodies were not affected by the reduced level of Atg8 (Figure 2.2C). These data suggest that even though Atg8 depends on Atg9 for its PAS localization, the role of Atg8 in autophagosome formation is distinct from that of Atg9, in that it specifically controls the size of autophagsomes.

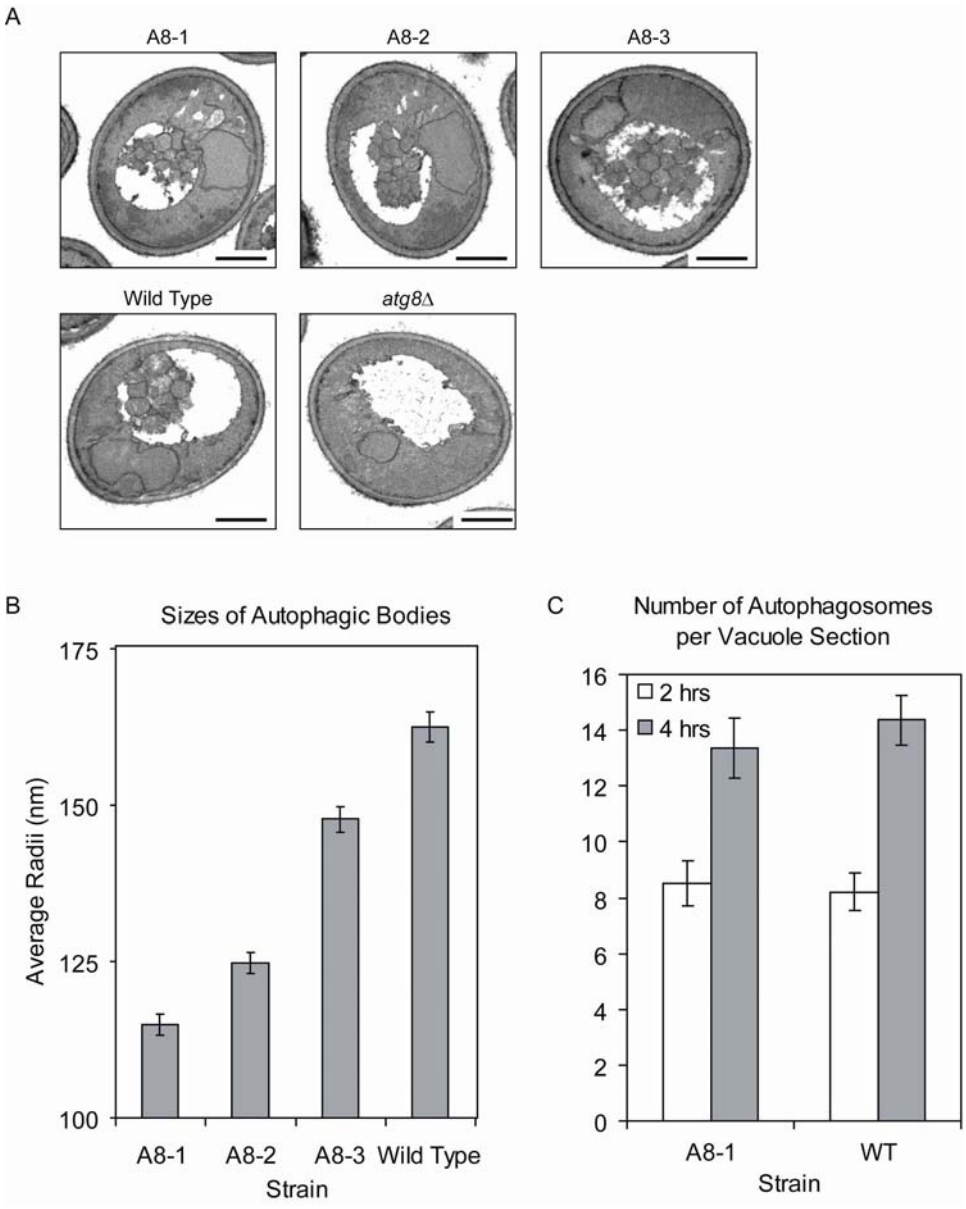

Figure 2.2 Atg8 controls the size of the autophagosome

(A, B) Lower amounts of Atg8 reduce the sizes of autophagosomes. Yeast cells were grown in rich medium to mid-log phase, then starved in nitrogen starvation medium for 4 h, fixed in potassium permanganate, and processed for electron microscopy (EM). (A) Representative EM images from *pep4*Δ strains. Autophagic bodies accumulated in A8-1, A8-2, A8-3, and wild-type background strains. No autophagic bodies were found in *atg8*Δ background cells. Scale bar, 1 μm. (B) Quantification of autophagic body size. The average radii of cross sections of autophagic bodies are shown; Error bar, S.E.M., n > 200. Autophagic bodies in the A8-1, A8-2 and A8-3 strains were significantly smaller than those of the wild-type (WT) background. (C) Atg8 level does not limit the number of auotphagosomes produced. Yeast cells starved for 2 and 4 h were collected and processed for EM. The average numbers of autophagic bodies per vacuole section are shown; Error bar, S.E.M., n > 100. Similar numbers of autophagic bodies were observed in strains with different amounts of Atg8.

The Dynamics of GFP-Atg8 during Autophagosome Formation

To gain further insight into how Atg8 participates in autophagosome formation, we used fluorescence microscopy to observe the dynamics of Atg8 in live cells. GFP-Atg8 was expressed under the control of the endogenous *ATG8* promoter in the *atg8Δ* background (strain GA8). When cells were examined under starvation conditions, we saw the constant emergence and disappearance of GFP-Atg8 punctate structures, each with a duration of approximately 10 minutes (Figure 2.3). The sizes of the GFP-Atg8 puncta expanded initially but then remained nearly the same when the fluorescence decreased (Figure 2.3).

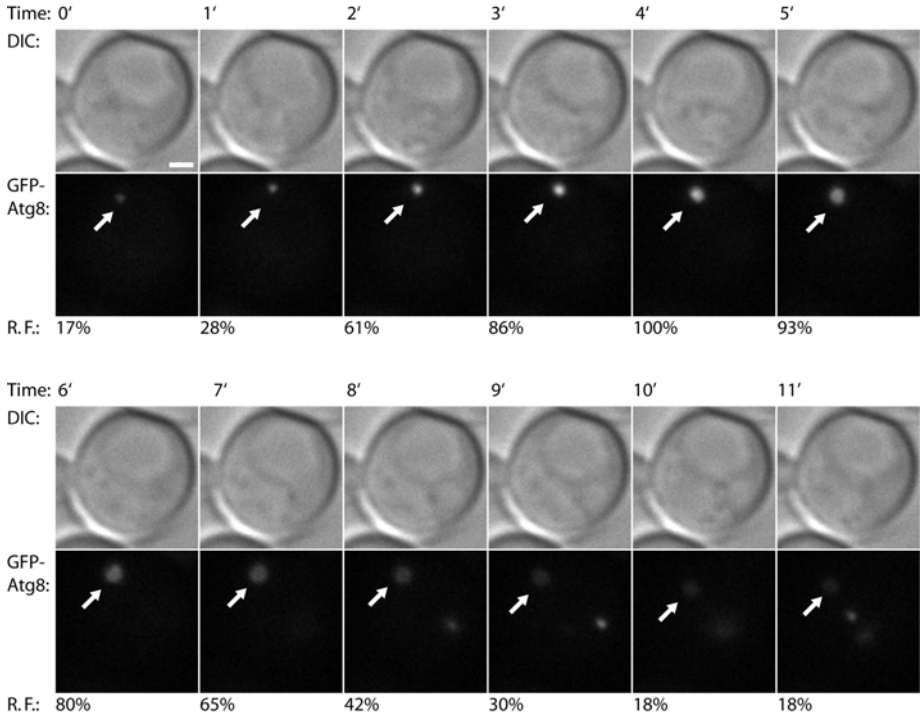

Figure 2.3 Tracing of one GFP-Atg8 punctum during autophagsome formation

Strain GA8 cells were starved for 1 h, immobilized on concanavalin A-treated cover slips, and incubated in starvation medium on a depression (concave) slide. Image stacks were collected every minute; only the images with GFP-Atg8 puncta (if present) in focus are shown. A GFP-Atg8 punctum expanded as the fluorescence increased and then retained that size as the fluorescence decreased. White arrows indicate the GFP-Atg8 punctum being tracked. During 15 minutes of observation, 90% cells displayed 1~4 such processes. R.F.: relative fluorescence normalized to peak value. DIC, differential interference contrast. Scale bar, 1 μm.

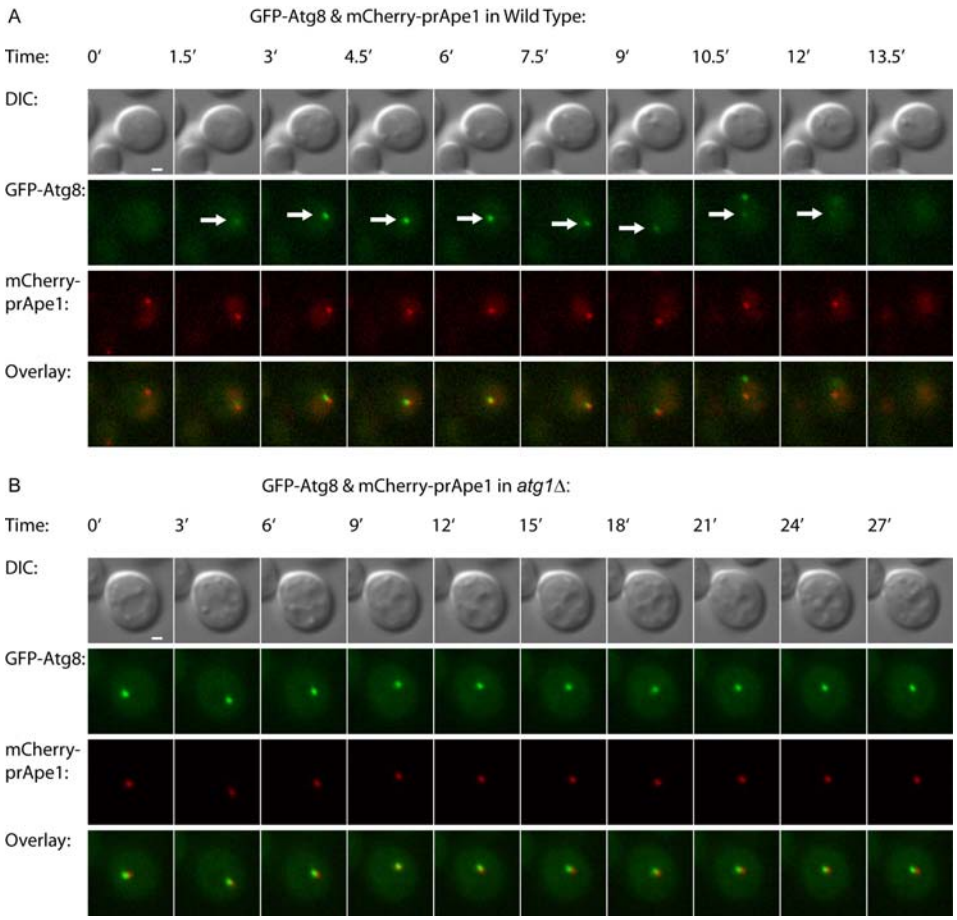

Figure 2.4 Dynamics of GFP-Atg8 during autophagosome formation

Yeast cells were grown in rich medium to mid-log phase, then starved for 1 h, and observed as in Figure 2.3. (A) The emergence and disappearance of GFP-Atg8 puncta correspond to autophagosome formation. GFP-Atg8 and mCherry-prApe1 were expressed under their endogenous promoters in wild-type cells. GFP-Atg8 was recruited to the PAS, marked by the presence of the cargo mCherry-prApe1; after some GFP-Atg8 was released, the cargo was delivered to the vacuole and disassembled. The white arrow indicates the GFP-Atg8 punctum being tracked. (B) The dynamic pattern is absent in *atg1*Δ cells. GFP-Atg8 and mCherry-prApe1 were expressed in *atg1*Δ cells. GFP-Atg8 and mCherry-prApe1 signals persisted without a significant decrease in fluorescence in their punctate structures during 30 min of observation. Scale bar, 1 μm.

To determine whether this dynamic pattern correlates with autophagosome formation, we repeated the analysis in cells expressing mCherry-prApe1 (Figure 2.4A) [35]. Precursor Ape1 forms a large oligomer in the cytosol, detectable as a single punctum, which becomes a cargo of an autophagosome in starvation conditions [32, 36]. Upon vacuolar delivery, the large oligomer disassembles into dodecamers, which then display a diffuse fluorescence pattern within the vacuole lumen. In wild-type cells, the disappearance of each mCherry-prApe1 punctum was preceded by the emergence and

disappearance of a colocalizing GFP-Atg8 punctum. In contrast, in *atg1Δ* cells, which are defective in autophagosome formation but not initial assembly of the PAS [6, 25, 37], both GFP-Atg8 and mCherry-prApe1 persisted without a significant decrease in fluorescence in punctate structures (Figure 2.4B). These data suggest that the dynamic pattern of Atg8 puncta formation and disassembly is an integral part of normal autophagy, and that it represents events that occur before the disassembly of the cargo complex in the vacuole.

The Majority of Atg8 at the PAS Is Released during Autophagosome Formation

To test if the decrease and disappearance of the GFP-Atg8 signal represents the degradation of GFP-Atg8-containing autophagic bodies in the vacuole, we examined the dynamics of GFP-Atg8 in *pep4Δ atg11Δ* cells (*ATG11* was knocked out to reduce the accumulation of Cvt bodies [38], which otherwise interfere in tracing the movement GFP-Atg8 punta that are associated with autophagic bodies). A decrease of the GFP-Atg8 signal was again clearly observed (Figure 2.5A). Following the decrease in GFP-Atg8 fluorescence, some GFP-Atg8 puncta persisted within the vacuole lumen, displaying a low amount of fluorescence, whereas the majority could no longer be detected. These data suggest that the majority of GFP-Atg8 molecules were released into the cytoplasm before autophagosome-vacuole fusion.

It should be noted that this large decrease of fluorescence was not an artifact due to photo-bleaching. We quantified the fluorescence of GFP-Atg8 punta in live cells and compared them against the values obtained from fixed cells. In fixed cells, photo-bleaching caused less than a 10% reduction in fluorescence after 5 minutes (Figure 2.5D). In contrast, in live *pep4Δ atg11Δ* cells and in GA8 cells, the fluorescence of GFP-Atg8 structures dropped well below 50% of the maximum intensities in 5 minutes post-peak (Figure 2.5B, C).

Next, we decided to test if the release of GFP-Atg8 fluorescence from the PAS required deconjugation. The deconjugation of Atg8—PE by Atg4 is necessary for normal autophagy [11], although its exact role is not clear. We expressed GFP-Atg8ΔR, which lacks the carboxyl terminal arginine residue (thus bypassing the first step of Atg4 processing), together with mCherry-prApe1 in *atg4Δ atg8Δ* cells. In the absence of Atg4,

Atg8ΔR can be conjugated normally but cannot be deconjugated. We then examined these cells in starvation conditions. As in wild-type cells, we found GFP-Atg8 puncta colocalizing with mCherry-prApe1, indicating that deconjugation is not required for the PAS localization of Atg8 (Figure 2.5E). However, these puncta did not show a significant decrease in fluorescence and the colocalizing mCherry-prApe1 remained visible (Figure 2.5E), suggesting that the release of GFP-Atg8 from the PAS that we are monitoring is mediated by Atg4 and that this reaction is a crucial step in autophagosome formation and/or completion.

Taken together, these results suggest that each cycle of appearance and disappearance of the GFP-Atg8 signal represents the recruitment and release of Atg8 involved in the formation and completion of an autophagosome.

The Amount of Atg8 at the PAS Regulates the Level of Autophagy

The PAS is generally considered to be the site where the core machinery proteins, including Atg8, act to form autophagosomes. We next tested whether the regulation of the level of autophagy that occurs through modulating the size of the autophagosome is accomplished by controlling the amount of Atg8 at the PAS. GFP-Atg8 was expressed in *atg8Δ* cells under the control of either its own promoter (strain GA8) or the promoter used in strain A8-1 (strain A81-GA8) (Figure 2.6A). After cells were incubated in starvation conditions for 1 hour, we quantified the peak fluorescence of the GFP-Atg8 PAS puncta during the dynamic cycles. The average intensity value in strain A81-GA8 was approximately 50% of that in strain GA8 (Figure 2.6B). Consistently, the Pho8Δ60 activity of strain A81-GA8 was lower than that of strain GA8 (Figure 2.6C), indicating that the amount of Atg8 recruited to the PAS regulates the level of autophagy.

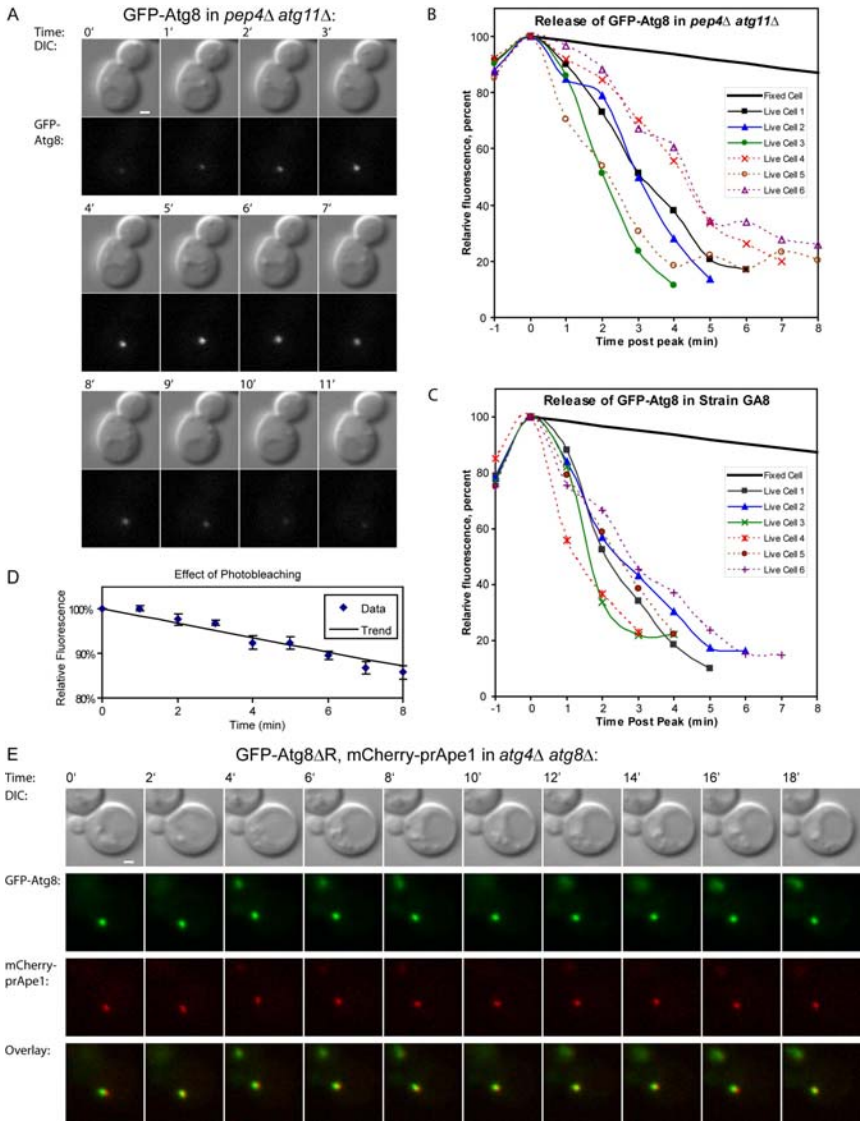

Figure 2.5 The majority of GFP-Atg8 at the PAS is released during autophagosome formation

(A) The decrease of signal intensity of GFP-Atg8 puncta is caused by the release of GFP-Atg8. GFP-Atg8 was expressed in *atg11*Δ *pep4*Δ cells. Yeast cells grown to mid-log phase in nutrient-rich medium were collected and starved in nitrogen-starvation medium for 30 min. Microscopy observation was performed as in Figure 2.4. The signal decreases were evident in *atg11*Δ *pep4*Δ cells, which are defective in degradation of autophagic bodies. (B, C, D) The significant decrease in fluorescence is not an artifact due to photobleaching. The intensities of GFP-Atg8 puncta in live cells and fixed cells were quantified. For live cells, the peak intensities were normalized as 100%, and the peaks were aligned to time 0. For fixed cells, the initial intensities were normalized as 100%. In fixed cells, photo-bleaching caused less than a 10% reduction in fluorescence after 5 min. In *atg11*Δ *pep4*Δ cells (B) and in strain GA8 (GFP-Atg8 in *atg8*Δ) (C), the remaining fluorescence at the PAS was clearly below 50% at 5 min post peak. The actual data from which the photobleaching trend line is generated is shown in (D). Error bar, S.E.M, n=6. (E) Atg8 deconjugation is required for the release of Atg8 and completion of autophagosomes. GFP-Atg8ΔR and mCherry-prApe1 were expressed in *atg4*Δ *atg8*Δ cells. Yeast cells were starved for 1 h. Microscopy observation was performed as in Figure 2.3. GFP-Atg8 and mCherry-prApe1 persisted in a punctate structure during 20 min of observation. Scale bar, 1 μm.

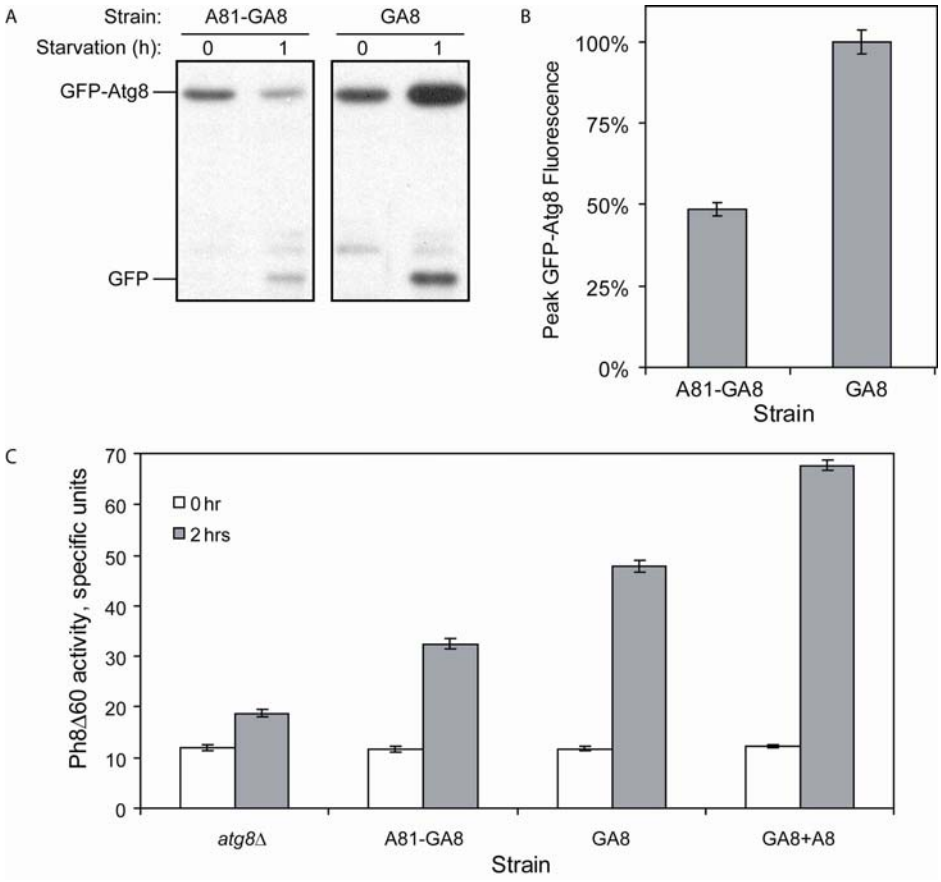

Figure 2.6 Amount of Atg8 at the PAS controls the level of autophagy

(A) Different amounts of GFP-Atg8 were expressed in strain A81-GA8 and GA8. GFP-Atg8 was expressed under the promoter used in strain A8-1 (strain A81-GA8) or its own promoter (strain GA8) in *atg8*Δ cells. Yeast cells were collected at the indicated time points after starvation. Protein extracts were analyzed by immunoblotting with anti-GFP antibody. GFP: GFP moiety, which is stable in the vacuole, released as the result of GFP-Atg8 degradation. (B) The amount of Atg8 recruited to the PAS is limited by the protein level. Yeast cells were starved in nitrogen-starvation medium for 1 h. Microscopy observation was performed as in Figure 2.4. Average peak intensities during dynamic cycles are shown. The average peak intensity in strain GA8 is normalized as 100%. Error bar, S.E.M., n > 100. Lower amounts of GFP-Atg8 were recruited to the PAS in strain A81-GA8 compared with strain GA8. (C) Autophagy levels in strain *atg8Δ*, A81-GA8, GA8, and GA8+A8. The Pho8Δ60 assay was performed as in Figure 2.1. Error bar, S.E.M. from three independent repeats.

Atg8 does not Control the Frequency of Autophagosome Formation

Our microscopy observation provided a novel method to test whether a lower amount of Atg8 limits the number of autophagosomes produced. Because the recruitment and release of the majority of Atg8 happens before the delivery of autophagosomes to the vacuole, the number of GFP-Atg8 signal peaks would reflect the number of autophagosomes formed. We compared the peak frequency in a strain (GA8) expressing

GFP-Atg8 alone with that in a strain (GA8+A8) expressing additional Atg8 (Figure 2.7A). In strain GA8, the average number of peaks per cell in 15 minutes was 2.2±0.1 (Mean ± S.E.M.). Strain GA8+A8 did not show a statistically significant difference in the frequency from strain GA8 (Figure 2.7B), even though the Pho8Δ60-dependent ALP activity was clearly higher in the former (Figure 2.7C), reflecting an increase in the total volume of the autophagosomes. This is consistent with our EM data, indicating that a lower amount of Atg8 did not limit the rate of autophagosome formation but did affect autophagosome volume. In contrast, the frequency was significantly lower in *atg27*Δ cells (Figure 2.7B), which are known to produce fewer autophagosomes and served as a control [34].

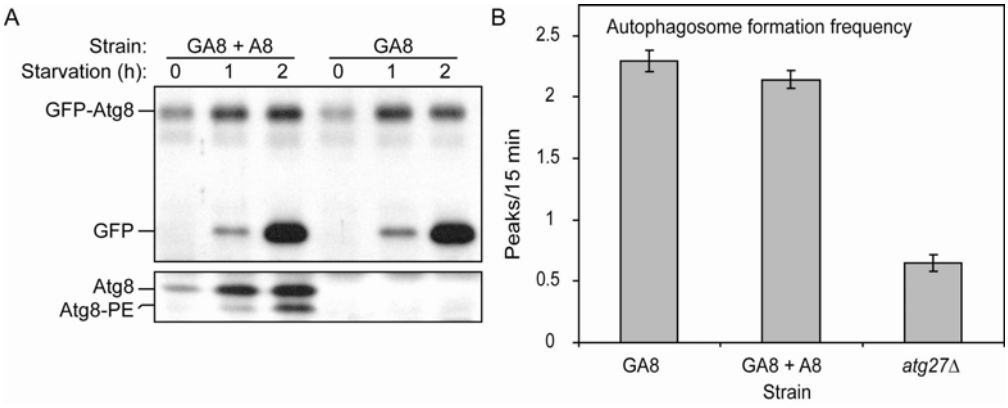

Figure 2.7 Atg8 does not control the frequency of autophagosome production

(A) GFP-Atg8 was expressed alone (strain GA8) or with additional Atg8 (strain GA8+A8). Samples were prepared as in Fig. 5 A. Protein extracts were analyzed by immunoblotting with anti-GFP antibody or anti-Atg8 antiserum. (B) Frequencies of autophagosome production in strains GA8 and GA8+A8 are comparable; the *atg27*Δ strain showed a significantly lower frequency. Yeast cells were starved for 1 h. The microscopy observation was performed as in Figure 2.4. The numbers of GFP-Atg8 peaks during 15 min were recorded. Error bar, S.E.M., n > 100. (C) Autophagy levels are different in strains GA8 and GA8+A8. The Pho8Δ60 assay was performed as in Figure 2.1. Error bar, S.E.M. from three independent repeats.

Discussion

In this study, we showed that (A) the amount of Atg8 regulates the level of autophagy by specifically modulating the size of the autophagosomes, whereas the number of autophagosomes is unaffected; (B) each round of autophagosome formation involves a cycle of Atg8 trafficking in which Atg8 is first recruited to an expanding structure and later released from it; (C) the release of Atg8 is essential for the completion

of autophagosome formation and it is mediated by deconjugation. In mammalian cells, the autophagosomes produced in response to group A *Streptococcus* invasion are larger than those seen in starvation conditions [39]. According to those data, where the signal is not saturated, the level of Atg8 induced by group A *Streptococcus* invasion is higher than that induced by starvation, suggesting that the regulation of autophagosome size achieved by controlling the amount of Atg8 may be a conserved mechanism.

For the first time, our data allowed temporal dissection of the autophagosome formation process based on real-time observations (Figure 2.4, 5). Here we propose a 5-stage model (Figure 2.8): In the first stage, cargos and factors required for the PAS recruitment of Atg8 arrive at the PAS; in stage 2, Atg8 arrives at the PAS and the Atg8-containing structure expands; stage 3 is a transitional step, allowing the completion of expansion and initiating release of Atg8 through deconjugation; in stage 4, additional Atg8 molecules are gradually released from the PAS; in stage 5, the phagophore matures into an autophagosome, and some Atg8 molecules are trapped inside. Previously, the lack of a data-derived multi-stage model restricted most studies on autophagosome formation to the PAS recruitment-dependency of autophagy-related proteins. Our model provides the foundation for re-analysis of the functions of known autophagy-related proteins and for screening new genes whose products act at each stage. In addition, this model serves as a reference point to coordinate the dynamics of other autophagy-related genes. For instance, it would be interesting to find at which stage Atg9, a protein known to cycle between the PAS and peripheral sites, departs from the PAS [24, 40].

Our results suggest that the expansion and deformation of the phagophore happens concurrently or slightly after the recruitment of Atg8 to the PAS, given that Atg8 is a causal factor in determination of autophagosome size. When Atg8 is released, the Atg8-containing structures retained their sizes (Figure 2.3), indicating that at this moment the expansion of the phagophore should be near completion, but not fully closed so that Atg8 molecules attached to the concave side of the phagophore (that will become the inner membrane of the autophagosome) can leave the membrane.

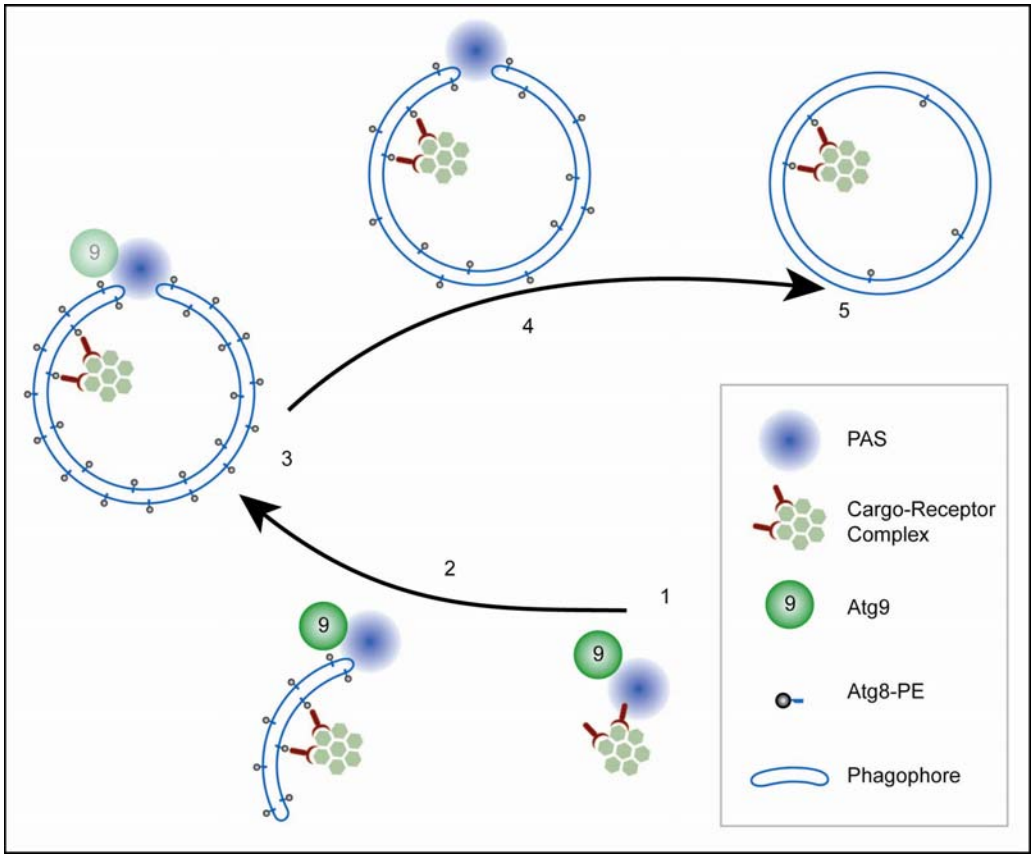

Figure 2.8 A multi-stage model of autophagosome formation

Stage 1, cargos and factors required for PAS recruitment of Atg8 (showing Atg9 as an example) arrive at the PAS. Stage 2, Atg8 arrives at the PAS and resides on an expanding structure, in coordination with the growth and deformation of the phagophore. Stage 3 is a transitional stage, marked by the completion of expansion and initiating the release of Atg8. Stage 4, additional Atg8 departs from the PAS. Stage 5, the phagophore matures into a completed autophagosome; only a small amount of Atg8 remains in the lumen. The timing of Atg9 departure is not yet determined.

At present, how Atg8 modifies the phagophore to produce different-sized autophagosomes is not clear. One possibility is that Atg8 is a component of a coat structure that supports the expansion and deformation of the phagophore. The amount of Atg8 at the PAS then decides the size of the coat structure and the autophagosome formed thereafter. At the end of the process, the coat structure is disassembled. Consistent with this model, Atg8 is known to interact with cargo receptors [36, 41], and its conjugation provides a natural link to the membrane. These properties are analogous to those of Sec24, an adaptor protein in the coat of COPII vesicles, which interacts with cargo receptors and the vesicle membrane while residing on the coat cage formed by heterotetramers of Sec13 and Sec31 [42, 43]. Another possibility is that Atg8 controls the

size of the phagophore by limiting membrane incorporation. Purified Atg8 can mediate liposome hemifusion *in vitro* [44]. In this model, the amount of Atg8 dictates the rate of phagophore expansion, and an independent mechanism will signal the end of expansion at a predetermined time point. At this moment, the edge of the phagophore will seek to merge with its opposing side. The determination of phagophore curvature is therefore a passive event instead of relying on an existing scaffold. Both models, however, are currently in need of critical supporting data. For the first model, even though the density of Atg8 molecules at the PAS may be consistent with a coat-like function (our unpublished data), the size of Atg8 is insufficient for connecting separate Atg8 proteins with each other; yet proteins that function analogously to Sec13 and Sec31 have not been identified. For the second model, it is not known whether the phagophore expands through vesicular fusion; and the localization of Atg8 at the planar region of the phagophore [26-28] is inconsistent with the proposed membrane incorporation site, along the growing edge [45].

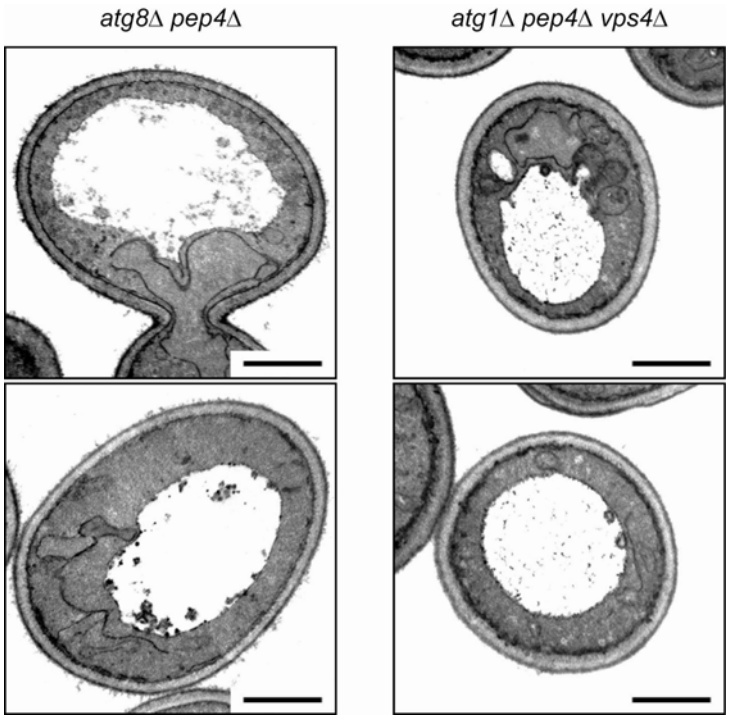

Figure 2.9 Vesicles of unknown identity are present in autophagy mutants

Samples were prepared for EM as in Figure 2.2. Occasionally, small vesicles were observed in the vacuoles of *atg8*Δ *pep4*Δ cells. Similar vesicles were also found in *atg1*Δ *pep4*Δ *vps4*Δ cells, which are defective in autophagosome formation. Scale bar, 1 μm.

Our data indicate that Atg8 is essential in autophagosome formation. In rare cases (in approximately 1% of the cells), however, small vesicular structures can be observed in *atg8*Δ *pep4*Δ cells (Figure 2.9). Previously, small autophagosome-like structures have also been detectd in *atg8*Δ cells [46]. Currently the identity of these structures cannot be tested in the absence of an autophagic membrane marker other than Atg8. In addition, similar rare structures can also be detected in *atg1*Δ *pep4*Δ *vps4*Δ cells, which are defective in autophagosome formation (Figure 2.9). Further experiments are needed to elucidate the nature of these vesicles.

Materials and Methods

Yeast Media

Rich medium (YPD): 1% yeast extract, 2% peptone, 2% glucose. Nitrogen starvation medium (SD-N): 2% glucose, 0.17% yeast nitrogen base without amino acids and ammonium sulfate.

Construction of Strains and Plasmids

Gene knockouts were performed as previously described [34]. To construct Atg8 expression plasmids, promoters from genes with protein levels expected to be similar to that of Atg8 in rich medium were placed in front of the *ATG8* open reading frame; the resulting Atg8 protein levels were tested by western blotting. Three plasmids were chosen for this study based on the following two criteria: (a) Atg8 amounts in starvation were lower than that of the wild-type strain, (b) Atg8 amounts in rich media were similar to that of the wild-type strain. Plasmid $pP_{ATG27}ATG8\text{-}406$ contains 740 bp of *ATG27* 5' sequence; plasmid $pP_{VPS30}ATG8\text{-}\ P_{ATG18}ATG8\text{-}406$ contains 420 bp of *VPS30* 5' sequence and 530 bp of *ATG18* 5' sequence in front of 2 copies of *ATG8* open reading frames, respectively; plasmid $pP_{ATG3}ATG8\text{-}406$ contains 380 bp of *ATG3* 5' sequence. Plasmid pP_{1K}*Green fluorescent protein (GFP)-ATG8-406* contains 990 bp of *ATG8* 5' sequence in front of GFP-Atg8 open reading frame. These Atg8 expressing plasmids or the corresponding empty vectors were linearized and integrated into the *atg8Δ* strain. The strains used in this study are listed in Table 2.1.

Table 2.1 Yeast strains used in this study

Descriptive Name	Strain Name	Genotype	Reference
Pho8Δ60 parent	TN124	MATα *leu2-3,112 trp1 ura3-52 pho8::pho8Δ60 pho13::LEU2*	[33]
	YZX200	TN124 *atg8Δ::KAN*	This study
atg8Δ	YZX231	TN124 *atg8Δ::KAN URA3 TRP1*	This study
Wild type	YXZ232	TN124 *URA3 TRP1*	This study
A8-1	YZX233	TN124 *atg8Δ::KAN* pP^{a}_{ATG27}*ATG8::URA3 TRP1*	This study
A8-2	YZX234	TN124 *atg8Δ::KAN* pP_{VPS30}*ATG8-*pP_{ATG18}*ATG8::URA TRP*	This study
A8-3	YZX235	TN124 *atg8Δ::KAN* pP_{ATG3}*ATG8::URA3 TRP1*	This study
Wild type *pep4Δ*	YZX213	TN124 *URA3 pep4Δ::TRP1*	This study
atg8Δ pep4Δ	YZX214	TN124 *atg8Δ::KAN URA3 pep4Δ::TRP1*	This study
A8-1 *pep4Δ*	YZX216	TN124 *atg8Δ::KAN* pP_{ATG27}*ATG8::URA3 pep4Δ::TRP1*	This study
A8-2 *pep4Δ*	YZX211	TN124 *atg8Δ::KAN* pP_{VPS30}*ATG8-*pP_{ATG18}*ATG8::URA3 pep4Δ::TRP1*	This study
A8-3 *pep4Δ*	YZX212	TN124 *atg8Δ::KAN* pP_{ATG3}*ATG8::URA3 pep4Δ::TRP1*	This study
GA8	YZX247	TN124 *atg8Δ::KAN* pP_{1K}*GFP-ATG8::URA3 TRP1*	This study
GFP-Atg8 mCherry-prApe1	YZX261	TN124 *atg8Δ::KAN* pP_{1K}*GFP-ATG8::URA3 Cherry-Ape1::TRP1*	This study
A81-GA8	YZX233	TN124 *atg8Δ::KAN* pP_{ATG27}*GFP-ATG8::URA3 TRP1*	This study
GA8+A8	YZX268	TN124 *atg8Δ::KAN* pP_{1K}*GFP-ATG8::URA3* pP_{ATG3}*ATG8::TRP1*	This study
atg1Δ pep4Δ vps4Δ	JHY28	SEY6210 *atg1Δ::HIS5 S.p. pep4Δ::LEU2 vps4Δ::TRP1*	[34]

[a] P, promoter

Electron Microscopy

Sample preparation and image acquisition were performed as described previously [34]. Autophagic body cross sections with a clear limiting membrane were outlined by hand using Adobe Photoshop. The area values of outlined autophagic body cross sections were obtained using the particle analysis function of ImageJ (http://rsb.info.nih.gov/ij/). The area values were then converted to radii for data presentation, using the formula: radius = square root of (area divided by pi).

Fluorescence Microscopy

Live cell fluorescence microscopy was performed as previously described [34] with the following modification: one side of the cover glass was coated with 1 mg/ml concanavalin A for 5 min, and rinsed with water; 100 μl of yeast cell culture was placed on the treated side for 3 min to immobilize yeast cells on the cover glass; the cover glass was rinsed with water, placed on a concavity slide containing liquid medium and observed under the microscope. Each experiment was repeated at least 3 times with more than 100 cells observed.

Quantification of Fluorescence Intensity

At each time point, a stack of images was collected along the z-axis to cover the entire cell. A projection of the image stack was created by calculating the sum of signal intensities. The intensity of GFP-Atg8 puncta was calculated as the difference between the absolute value of the GFP-Atg8 punctum and that of the local background, using the intensity of its adjacent area, as determined with softWoRx® software (Applied Precision, LLC, Issaquah, WA).

Additional Assays

The protein extraction, immunoblot and alkaline phosphatase (Pho8Δ60) assays were performed as described previously [33, 34].

References

1. Xie Z, Klionsky DJ. Autophagosome formation: core machinery and adaptations. Nat Cell Biol 2007; 9:1102-9.

2. Levine B, Klionsky DJ. Development by self-digestion: molecular mechanisms and biological functions of autophagy. Dev Cell 2004; 6:463-77.

3. Shintani T, Klionsky DJ. Autophagy in health and disease: a double-edged sword. Science 2004; 306:990-5.

4. Boland B, Nixon RA. Neuronal macroautophagy: from development to degeneration. Mol Aspects Med 2006; 27:503-19.

5. Schmid D, Münz C. Innate and adaptive immunity through autophagy. Immunity 2007; 27:11-21.

6. Suzuki K, Kirisako T, Kamada Y, Mizushima N, Noda T, Ohsumi Y. The pre-autophagosomal structure organized by concerted functions of *APG* genes is essential for autophagosome formation. Embo J 2001; 20:5971-81.

7. Kim J, Huang W-P, Stromhaug PE, Klionsky DJ. Convergence of multiple autophagy and cytoplasm to vacuole targeting components to a perivacuolar membrane compartment prior to de novo vesicle formation. J Biol Chem 2002; 277:763-73.

8. Yorimitsu T, Klionsky DJ. Autophagy: molecular machinery for self-eating. Cell Death Differ 2005; 12 Suppl 2:1542-52.

9. Ichimura Y, Kirisako T, Takao T, Satomi Y, Shimonishi Y, Ishihara N, Mizushima N, Tanida I, Kominami E, Ohsumi M, Noda T, Ohsumi Y. A ubiquitin-like system mediates protein lipidation. Nature 2000; 408:488-92.

10. Paz Y, Elazar Z, Fass D. Structure of GATE-16, membrane transport modulator and mammalian ortholog of autophagocytosis factor Aut7p. J Biol Chem 2000; 275:25445-50.

11. Kirisako T, Ichimura Y, Okada H, Kabeya Y, Mizushima N, Yoshimori T, Ohsumi M, Takao T, Noda T, Ohsumi Y. The reversible modification regulates the membrane-binding state of Apg8/Aut7 essential for autophagy and the cytoplasm to vacuole targeting pathway. J Cell Biol 2000; 151:263-76.

12. Kim J, Huang W-P, Klionsky DJ. Membrane recruitment of Aut7p in the autophagy and cytoplasm to vacuole targeting pathways requires Aut1p, Aut2p, and the autophagy conjugation complex. J Cell Biol 2001; 152:51-64.

13. Hemelaar J, Lelyveld VS, Kessler BM, Ploegh HL. A single protease, Apg4B, is specific for the autophagy-related ubiquitin-like proteins GATE-16, MAP1-LC3, GABARAP, and Apg8L. J Biol Chem 2003; 278:51841-50.

14. Tanida I, Mizushima N, Kiyooka M, Ohsumi M, Ueno T, Ohsumi Y, Kominami E. Apg7p/Cvt2p: A novel protein-activating enzyme essential for autophagy. Mol Biol Cell 1999; 10:1367-79.

15. Tanida I, Tanida-Miyake E, Ueno T, Kominami E. The human homolog of *Saccharomyces cerevisiae* Apg7p is a Protein-activating enzyme for multiple substrates including human Apg12p, GATE-16, GABARAP, and MAP-LC3. J Biol Chem 2001; 276:1701-6.

16. Tanida I, Tanida-Miyake E, Komatsu M, Ueno T, Kominami E. Human Apg3p/Aut1p homologue is an authentic E2 enzyme for multiple substrates, GATE-16, GABARAP, and MAP-LC3, and facilitates the conjugation of hApg12p to hApg5p. J Biol Chem 2002; 277:13739-44.

17. Hanada T, Noda NN, Satomi Y, Ichimura Y, Fujioka Y, Takao T, Inagaki F, Ohusmi Y. The ATG12-ATG5 conjugate has a novel E3-like activity for protein lipidation in autophagy. J Biol Chem 2007.

18. Mizushima N, Noda T, Yoshimori T, Tanaka Y, Ishii T, George MD, Klionsky DJ, Ohsumi M, Ohsumi Y. A protein conjugation system essential for autophagy. Nature 1998; 395:395-8.

19. Mizushima N, Sugita H, Yoshimori T, Ohsumi Y. A new protein conjugation system in human. The counterpart of the yeast Apg12p conjugation system essential for autophagy. J Biol Chem 1998; 273:33889-92.

20. Kuma A, Mizushima N, Ishihara N, Ohsumi Y. Formation of the approximately 350-kDa Apg12-Apg5.Apg16 multimeric complex, mediated by Apg16 oligomerization, is essential for autophagy in yeast. J Biol Chem 2002; 277:18619-25.

21. Mizushima N, Kuma A, Kobayashi Y, Yamamoto A, Matsubae M, Takao T, Natsume T, Ohsumi Y, Yoshimori T. Mouse Apg16L, a novel WD-repeat protein, targets to the autophagic isolation membrane with the Apg12-Apg5 conjugate. J Cell Sci 2003; 116:1679-88.

22. Kametaka S, Okano T, Ohsumi M, Ohsumi Y. Apg14p and Apg6/Vps30p form a protein complex essential for autophagy in the yeast, *Saccharomyces cerevisiae*. J Biol Chem 1998; 273:22284-91.

23. Reggiori F, Shintani T, Nair U, Klionsky DJ. Atg9 cycles between mitochondria and the pre-autophagosomal structure in yeasts. Autophagy 2005; 1:101-9.

24. Young ARJ, Chan EYW, Hu XW, Kochl R, Crawshaw SG, High S, Hailey DW, Lippincott-Schwartz J, Tooze SA. Starvation and ULK1-dependent cycling of mammalian Atg9 between the TGN and endosomes. J Cell Sci 2006; 119:3888-900.

25. Suzuki K, Kubota Y, Sekito T, Ohsumi Y. Hierarchy of Atg proteins in pre-autophagosomal structure organization. Genes Cells 2007; 12:209-18.

26. Kirisako T, Baba M, Ishihara N, Miyazawa K, Ohsumi M, Yoshimori T, Noda T, Ohsumi Y. Formation process of autophagosome is traced with Apg8/Aut7p in yeast. J Cell Biol 1999; 147:435-46.

27. Kabeya Y, Mizushima N, Ueno T, Yamamoto A, Kirisako T, Noda T, Kominami E, Ohsumi Y, Yoshimori T. LC3, a mammalian homologue of yeast Apg8p, is localized in autophagosome membranes after processing. EMBO J 2000; 19:5720-8.

28. Kabeya Y, Mizushima N, Yamamoto A, Oshitani-Okamoto S, Ohsumi Y, Yoshimori T. LC3, GABARAP and GATE16 localize to autophagosomal membrane depending on form-II formation. J Cell Sci 2004; 117:2805-12.

29. Huang W-P, Scott SV, Kim J, Klionsky DJ. The itinerary of a vesicle component, Aut7p/Cvt5p, terminates in the yeast vacuole via the autophagy/Cvt pathways. J Biol Chem 2000; 275:5845-51.

30. Tanida I, Minematsu-Ikeguchi N, Ueno T, Kominami E. Lysosomal turnover, but not a cellular level, of endogenous LC3 is a marker for autophagy. Autophagy 2005; 1:84-91.

31. Klionsky DJ, Cuervo AM, Seglen PO. Methods for monitoring autophagy from yeast to human. Autophagy 2007; 3:181-206.

32. Baba M, Osumi M, Scott SV, Klionsky DJ, Ohsumi Y. Two distinct pathways for targeting proteins from the cytoplasm to the vacuole/lysosome. J Cell Biol 1997; 139:1687-95.

33. Noda T, Matsuura A, Wada Y, Ohsumi Y. Novel system for monitoring autophagy in the yeast *Saccharomyces cerevisiae*. Biochem Biophys Res Commun 1995; 210:126-32.

34. Yen W-L, Legakis JE, Nair U, Klionsky DJ. Atg27 is required for autophagy-dependent cycling of Atg9. Mol Biol Cell 2007; 18:581-93.

35. Shaner NC, Campbell RE, Steinbach PA, Giepmans BN, Palmer AE, Tsien RY. Improved monomeric red, orange and yellow fluorescent proteins derived from Discosoma sp. red fluorescent protein. Nat Biotechnol 2004; 22:1567-72.

36. Shintani T, Huang W-P, Stromhaug PE, Klionsky DJ. Mechanism of cargo selection in the cytoplasm to vacuole targeting pathway. Dev Cell 2002; 3:825-37.

37. Tsukada M, Ohsumi Y. Isolation and characterization of autophagy-defective mutants of *Saccharomyces cerevisiae*. FEBS Lett 1993; 333:169-74.

38. Shintani T, Klionsky DJ. Cargo proteins facilitate the formation of transport vesicles in the cytoplasm to vacuole targeting pathway. J Biol Chem 2004; 279:29889-94.

39. Nakagawa I, Amano A, Mizushima N, Yamamoto A, Yamaguchi H, Kamimoto T, Nara A, Funao J, Nakata M, Tsuda K, Hamada S, Yoshimori T. Autophagy defends cells against invading group A *Streptococcus*. Science 2004; 306:1037-40.

40. Reggiori F, Tucker KA, Stromhaug PE, Klionsky DJ. The Atg1-Atg13 complex regulates Atg9 and Atg23 retrieval transport from the pre-autophagosomal structure. Dev Cell 2004; 6:79-90.

41. Pankiv S, Clausen TH, Lamark T, Brech A, Bruun JA, Outzen H, Øvervatn A, Bjørkøy G, Johansen T. p62/SQSTM1 binds directly to Atg8/LC3 to facilitate

degradation of ubiquitinated protein aggregates by autophagy. J Biol Chem 2007; 282:24131-45.

42. Lederkremer GZ, Cheng Y, Petre BM, Vogan E, Springer S, Schekman R, Walz T, Kirchhausen T. Structure of the Sec23p/24p and Sec13p/31p complexes of COPII. Proc Natl Acad Sci U S A 2001; 98:10704-9.

43. Gurkan C, Stagg SM, Lapointe P, Balch WE. The COPII cage: unifying principles of vesicle coat assembly. Nat Rev Mol Cell Biol 2006; 7:727-38.

44. Nakatogawa H, Ichimura Y, Ohsumi Y. Atg8, a ubiquitin-like protein required for autophagosome formation, mediates membrane tethering and hemifusion. Cell 2007; 130:165-78.

45. Kovács AL, Palfia Z, Réz G, Vellai T, Kovacs J. Sequestration revisited: integrating traditional electron microscopy, de novo assembly and new results. Autophagy 2007; 3:655-62.

46. Abeliovich H, Dunn WA, Jr., Kim J, Klionsky DJ. Dissection of autophagosome biogenesis into distinct nucleation and expansion steps. J Cell Biol 2000; 151:1025-34.

Chapter 3
Statistical Methods for Estimating the Sizes of Intracellular Vesicles from Electron Microscopy Data

Abstract

Assessing the sizes of original vesicles from the 2-D images is an important component of electron microscopy studies. Although the collective properties, such as total volume or total surface area, can be obtained directly from the random sections, it is difficult to estimate the sizes of individual objects. For a population of vesicles heterogeneous in size, random sectioning results in size-biased sampling. Here I developed two methods for estimating the sizes of intracellular vesicles from size-biased data. One method uses computer programming to simulate the random sectioning of aggregated vesicles. The second method simplifies the process by using numerical integration without considering vesicle aggregation. Both methods can be applied to establish the correlation between the size distribution of the vesicles and that of vesicle sections and to subsequently estimate the sizes of autophagic bodies from real sectioning data. The two methods were used to calculate the area density of Atg8 molecules at the phagophore assembly site. The result suggested that the area density of Atg8 at the PAS is comparable with that of proteins that forms the COPII coat.

The Computational Simulation Method

Macroautophagy, hereafter referred to as autophagy, is a pivotal intracellular degradation process[1]. During autophagy, cytoplasmic materials are sequestered into an expanding membrane sac, the phagophore, which latter matures into a double membrane vesicle, the autophagosome. Each autophagosome eventually fuses with a lysosome, leading to the degradation of the inner membrane and the cargos. The formation of autophagosomes is catalyzed by a set of core machinery proteins at the phagophore assembly site (PAS). The core machinery is supplemented by certain auxiliary proteins, the composition of which varies depending on physiological stimuli.

Although autophagosomes and vesicles of the secretory pathway share similar mechanisms in their fusion with their corresponding destination compartments[2, 3], it is not clear whether the formation processes of autophagosomes and secretory vesicles also follow the same principle. It is generally accepted that vesicles in the secretory pathway are generated from existing membrane structures by budding[4]. This involves the deformation of the membrane by the coat complexes, such as the COPII coat for endoplasmic reticulum (ER) to Golgi complex transport, the COPI coat in retrograde intra-Golgi complex and Golgi complex to ER transport, and the clathrin coat in post-Golgi transport[5]. Although the participating components vary, these coats share a two-layer scheme of organization, with a membrane proximal layer of adaptor proteins and a membrane distal layer of cage proteins. The assembly and disassembly of the coats are regulated by small GTPases. In autophagosome formation, however, the phagophore is considered to be formed *de novo* through membrane expansion instead of budding from existing organelles[6]. A Sar1-like GTPase, which can be targeted to prevent coast disassembly, is absent from the currently known molecular machinery of autophagosome formation. It is therefore unknown whether the determination of the curvature of the phagophore involves a coat cage.

Recently, we discovered that a member of the core autophagosome formation machinery, Atg8, specifically controls the sizes of autophagosomes[7]. Atg8 is a ubiquitin-like protein[8, 9]. Although it has been suggested to be a tethering factor based on *in vitro*

results[10], properties of Atg8 revealed by *in vivo* studies possess strong resemblance to those of coat adaptor proteins. During autophagosome formation, Atg8 is conjugated to phosphatidylethanolamine (PE) and initially resides on the surface of the phagophore[11, 12]. Later, the majority of Atg8 needs to be released by deconjugation prior to the completion of autophagosome formation[7], which mirrors the de-coating stage. Similar to known coat adaptors, Atg8 also interacts with cargo receptors[13, 14]. Because the phagophore is a membrane sac with two layers of membrane in its planar regions, a transmembrane cargo receptor similar to those in the secretory pathway will not be able to reach coat adaptors on the convex side. This may explain why, unlike other coat adaptors, Atg8 localizes to both sides of the phagophore, with the population on the concave side presumably responsible for interacting with cargo receptor proteins. Functioning as a coat adaptor, Atg8 may restrict the size of the coat cage by limiting the amounts of cage proteins recruited. If this is the case, even though Atg8 does not form a cage by itself, the area density of Atg8 molecules on the membrane should be comparable to that of cage elements. Therefore I tested the coat adaptor model by estimating the area density of Atg8 on the phagophore.

The area density of Atg8 was calculated using two input values: (1) the number of Atg8 molecules recruited to the PAS and (2) the size of the autophagosome, which should correspond to the size of the fully expanded phagophore. Our laboratory recently measured the number of Atg8 molecules recruited to the PAS by fluorescence microscopy using GFP-tagged Atg8 expressed in *atg8Δ* cells under the control of endogenous *ATG8* promoter. Under nitrogen starvation conditions, the average peak number of GFP-Atg8 molecule in each round of Atg8 recruitment and release is found to be approximately 272±9 (mean ± S.E.M., n=100) (Table 3.1) (Geng J. *et. al*, in press).

I then used electron microscopy to estimate the sizes of autophagosomes. When the *PEP4* gene encoding the vacuolar aspartyl protease Pep4 is knocked out, the inner single-membrane vesicle of autophagosomes, termed autophagic bodies, can be preserved in the yeast vacuole (a lysosome analogue) and be visualized easily in transmission electron microscopy (Figure 3.1). The average radius of autophagic body cross sections in *pep4Δ* cells from the aforementioned GFP-Atg8-expressing strain is 127±2 nm (mean ± S.E.M., n>200) (Table 3.1).

Table 3.1 Summary of results in the estimation of the area density of Atg8

Estimation of GFP-Atg8 Density		
Number of GFP-Atg8 molecules at the PAS	Mean	S.E.M. (n=100)
	272	9
Radii of autophagic body sections	Mean	S.E.M. (n>200)
	127 nm	2 nm
Radii of autophagic bodies	Mean	C.I.
	148 nm	5 nm
Area density of GFP-Atg8	1 per $2x10^3$ nm^2	
Length of edge	40~50 nm	

S.E.M., standard error of the mean. C.I., 95% confidence interval.

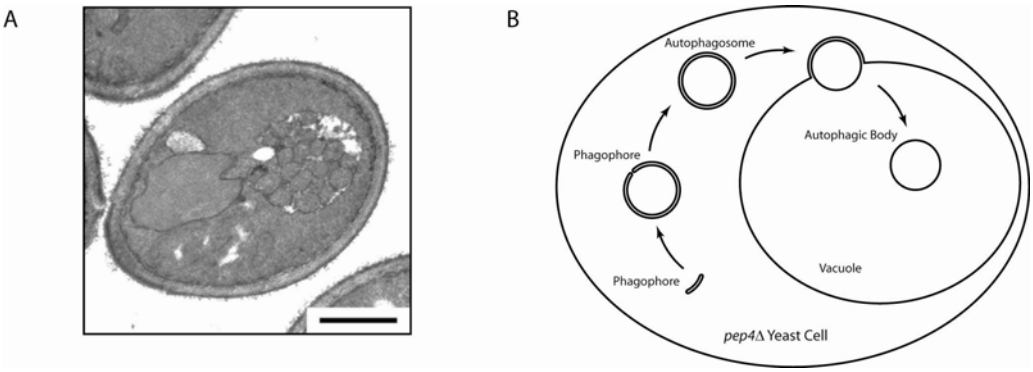

Figure 3.1 Autophagic bodies in *pep4Δ* cells

(A) A representative section of a yeast cell. *atg8Δ pep4Δ* cells expressing GFP-Atg8 grown to mid-log phase were incubated in nitrogen starvation medium for 4 hours and processed for electron microscopy. Autophagic bodies accumulated as a cluster of single membrane vesicles in the yeast vacuole. Scale bar, 1 μm. (B) The formation of autophagic bodies. When autophagosomes fuse with the vacuole, the inner vesicles are released into the vacuole lumen. They are termed autophagic bodies. In *pep4Δ* cells, autophagic bodies are not degraded.

To calculate the actual sizes of these vesicles, however, the biases introduced by the sectioning process need to be corrected. When sectioning a spherical object, the radii of most sections are smaller than that of the sphere, contributing a negative bias. In a population of spheres heterogeneous in size, larger ones have higher probabilities of getting sectioned, contributing a positive bias. In addition to these two major biases, two

minor biases are introduced by the following factors: (1) the aggregation of autophagic bodies will obscure each other on the overlaid areas (Figure 3.1A); (2) cross sections below a certain size threshold are difficult to recognize because they do not have sufficient details to be distinguished from the background noise.

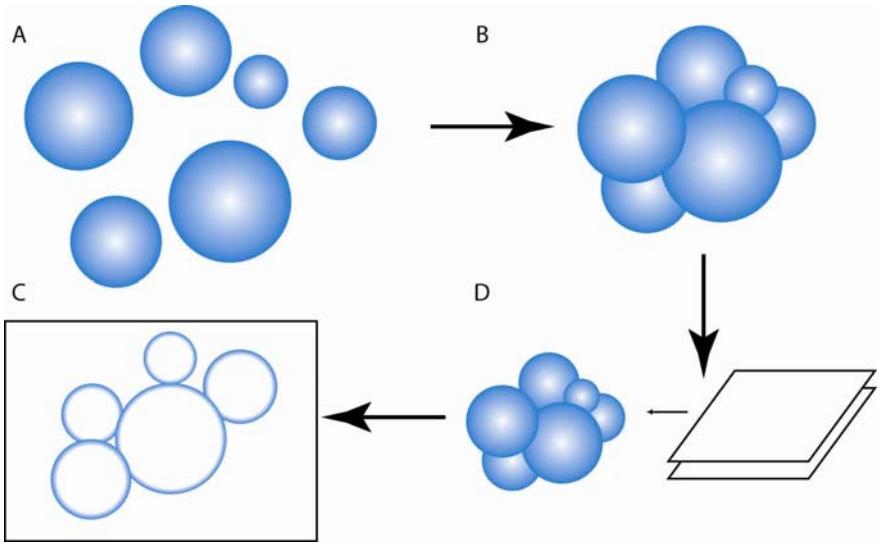

Figure 3.2 Scheme for the computational simulation of sectioning autophagic bodies

(A) First, the program generates a population of vesicles based on the specified parameters. (B)Then, the vesicles are positioned so that their surfaces contact each other. (C) The vesicle cluster is sectioned to produce a 70 nm-thick slice. (D) The areas of vesicle sections in the slice is quantified and reported.

Although similar problems have been studied in the past, I was unable to find a suitable analytical solution. Instead, I developed a computational method in collaboration with Mr. Maciej B. Szefler and Dr. Edwards D. Rothman (Dept. of Statistics, UM). The code was written using the R statistical software environment (http://www.r-project.org/) according to the following assumptions (Figure 3.2) (The source code can be download here: http://www-personal.umich.edu/~zxie/Research/Statistical Tools.htm): (a) autophagic bodies are nearly rigid spheres; (b) radii of autophagic bodies are distributed log-normally with unknown parameters, μ and σ, which correspond to the mean and standard deviation of the distribution at a log scale; (c) accumulated autophagic bodies are positioned so that their surfaces are in contact with each other; (d) the thickness of each sample section is 70 nm; (e) cross sections with radii less than 50 nm (the recognition threshold in my own experience) are ignored. The simulation process first

generates a set of vesicles *in silico* based on the distribution with a given set of μ and σ values. Next, these vesicles are rearranged to be in contact with each other using an algorithm described by Milenkovic[15]. The pile of vesicles is then sectioned, *in silico*, to produce a 70 nm thick slice, and areas of vesicle cross sections are reported. By varying the parameters of the original distribution, the correlation between the observed cross section distribution and the original distribution can be established by linear regression using the empirical moments.

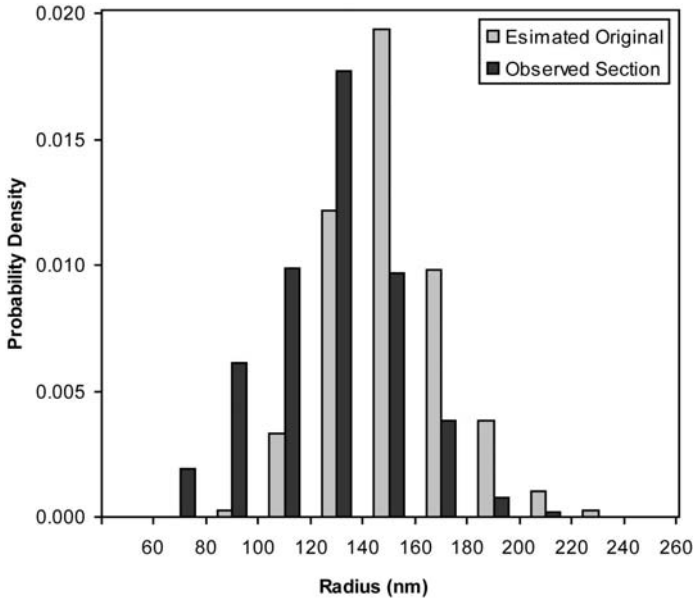

Figure 3.3 The size distributions of observed sections and estimated original vesicles

Observed section, sizes of actually observed sections of autophagic bodies. Estimated original, the sizes of original autophagic bodies estimated from simulation results.

Using this method, I estimated the original autophagic body radii distribution using the data from the electron microscopy analyses (Figure 3.3). The estimated average radius was 148±5 nm (mean ± 95% confidence interval) (Table 3.1). Assume that GFP-Atg8 is distributed evenly on both the convex and concave sides of the phagophore, the result above translates into one Atg8 molecule per $2x10^3$ nm^2 of surface area (Table 3.1). If each Atg8 molecule resides on a vertex of a polyhedral cage, the corresponding length of the edge will be approximately 40~50 nm, and the exact value will depend on the

composition of the polyhedron. In comparison, the length of the COPII coat edge is approximately 30 nm[16].

My result suggests that a coat adapter role for Atg8 remains a possibility. The key missing piece in the model, however, is the identity of components that constitute the edge of the coat. Previously, the complex formed by Atg12, Atg5 and Atg16 was proposed to be a coat candidate[17]. However, the number of Atg16 molecules recruited to the PAS is one order of magnitude lower than that of Atg8 (Geng J. *et. al*, in press), ruling out the possibility that the complex can fully cover the phagophore by itself. The function of Atg12—Atg5-Atg16 may instead be limited to recruiting Atg8 and facilitating Atg8 conjugation[18-22].

The Excel Numerical Integration Method

Although the computational simulation method solved the problem of estimating sizes of vesicles, I realize that it has two limitations. The first one is the speed. The program can produce approximately 300 sections of vesicles for a set of μ and σ in an hour. In order to use linear regression, one would need to try about 10 or more sets of μ and σ, which means a whole day of computational work. The second one is accessibility. Whereas the R software is familiar to most researchers in statistics, it is not yet widely used by biologists. Currently, I am working with LSI IT staff to set up a server to run the program with an easy-to-use web interface. This will eliminate the need to learn the R software. The problem of speed, however, is intrinsic to the method.

I then designed a second method that tackles both issues: speed and ease of use. This is a method implemented in Microsoft Excel®. It runs numerical integration in the background. To simplify the process, it ignores any obscuring of vesicles by other vesicles close by. Similar to the first method, the overall concept is to establish the correlation between the size distribution of vesicles and that of sections of vesicles. Here, I present steps to use this method first and the mathematical background afterwards. The descriptions are tailored for the exemplary spreadsheet file, which can be downloaded from http://www-personal.umich.edu/~zxie/Research/Statistical Tools.htm .

Firstly, to set the empirical parameters: the thickness of the sample slice (generally around 70 nm) and the size thresholds for recognizable vesicle sections (Figure 3.4). In reality, when vesicle sections get small enough, I can not recognize them reliably. The upper threshold is where it becomes difficult to recognize. The lower threshold is where it becomes impossible to recognize.

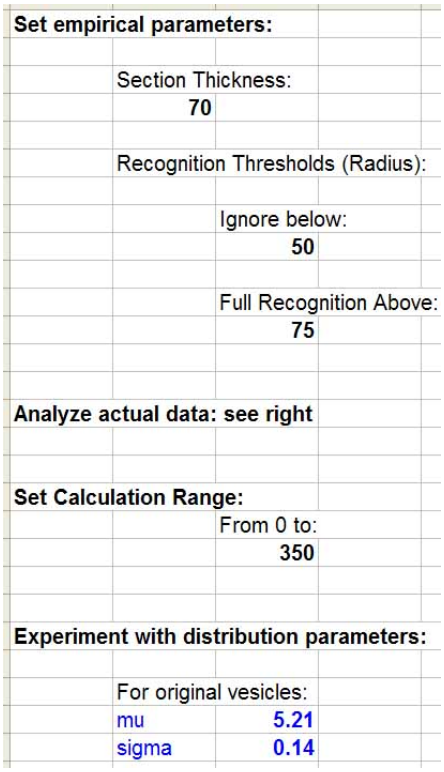

Figure 3.4 Entering parameters in the spread sheet

A screen shot showing the region in the spread sheet where the user specify analysis parameters: Section Thickness, Recognition Thresholds, Calculation Range, μ and σ.

Next, to analyze the actual data (Figure 3.5). Once the area values are converted to radii, calculate the following: mean, standard deviation, skewness, and kurtosis (the corresponding Excel functions are AVERAGE(), STDEV(), SKEW(), and KURT()). It is also preferable to plot the probability density of the actual data (Figure 3.6). The density plot provides a graphical view of the actual data to compare with theoretical data generated later.

Third step is to choose a calculation range (Figure 3.4). Vesicles below this range are considered in the calculation. As a starting point, set it to be 1.5 times of (mean + 2 standard deviations). This range need to be increased later if it can not cover the majority part of the size distribution.

Actual Data:			Analysis:				
	Area (nm^2)			Mean		Skewness	
		Radius (nm)			Standard Deviation		Kurtosis
	85611	165		161.6	40.3	-0.0706	-0.06722
	44189	119					
	36767	108		Sample Number			
	68167	147		430			
	24556	88					

Figure 3.5 Analyzing the actual data

A screen shot showing the region in the spread sheet where actual data are analyzed. Four values are calculated using the built-in functions: Mean, Standard Deviation, Skewness, Kurtosis.

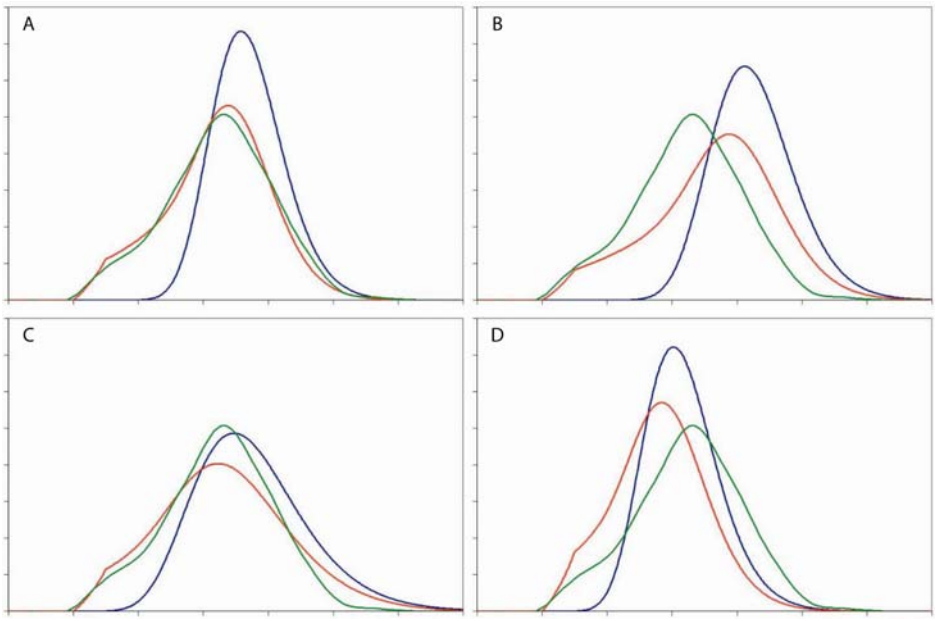

Figure 3.6 Experimenting with distribution parameters for a good fit to the actual data

Shown here are the probability density plots for the following size distributions: green line, actually observed sections; blue line, theoretical original vesicles; red line, theoretical sections of vesicles. By changing the parameters μ and σ for the theoretical original vesicles (blue line), a user can try to fit the theoretical section result (red line) to the actual one (green line). (A) A good fit. (B) Bigger than actual. (C) Wider than actual. (D) Smaller than actual.

Fourth step, to experiment with the parameters of the size distribution of the original vesicles and collect the theoretical data of resulted vesicle sections (Figure 3.6).

The two parameters μ and σ can be viewed as the mean and the standard deviation of the original distribution at a log scale. Ideally the user want to use the parameter close to the real value of the sample, so to have a graphical plot of actual data is advantageous because the user can find a good visual fit first and only try values around that pair of μ and σ (Figure 3.6). For instance, if μ = 5.21 with σ = 0.15 provides a good fit, the user can try μ = 5.16, 5.21, 5.26 versus σ = 0.11, 0.15, 0.19, a total of 9 combinations. For each set of μ and σ, the user should record μ and σ^2 of the original distribution together with the mean, standard deviation, skewness, and kurtosis of the calculated section size distribution.

Last step, to estimate the parameters of size distribution of the original vesicles. Run a linear regression using the sets of results collected in the previous step and the mean, standard deviation, skewness, kurtosis of the actual data. After obtaining μ and σ^2, the corresponding mean and standard deviation of the original radii are then calculated as:

$$\text{Original mean} = e^{\mu+\frac{\sigma^2}{2}}$$

$$\text{Original standard deviation} = \sqrt{(e^{\sigma^2}-1)e^{2\mu+\sigma^2}}$$

In the example file, I chose the following settings: slice thickness 70 nm, size thresholds 50 and 75 nm, calculation range 350 nm. Of 430 autophagic body cross sections from *pep4Δ* yeast, the mean radius is 162 nm; the standard deviation is 40 nm. From these data the sizes of the original autophagic bodies are estimated, the mean radius is 188 nm, and the standard deviation is 26 nm.

Estimating vesicle sizes from random vesicle sections is a classical stereological problem. Assuming (1) vesicles are spherical, and r(x) is the probability density function of vesicle radii; (2) vesicles are randomly positioned in space, resulting in size biased sampling when taking a random slice of the space; (3) the thickness is the sample slice is 2t; then the density function of the radii of the projected vesicle sections s(y) is a function of r()[23]:

$$\mathrm{s}(y) = \frac{t}{t+\int_0^\infty x\,\mathrm{r}(x)\,\mathrm{d}\,x}\mathrm{r}(y) + \int_y^\infty \frac{x\,\mathrm{r}(x)}{t+\int_0^\infty x\,\mathrm{r}(x)\,\mathrm{d}\,x}\frac{y}{x\sqrt{x^2-y^2}}\mathrm{d}\,x\text{, for y>0}$$

For a given piece of vesicle cross section, whether it can be reliably recognized and collected as data is affected by its size. In practice, very small ones are generally not collected. Assuming below a lower threshold l all are ignored, above an upper threshold u all are collected, and in between the possibility of being collected is proportional to the size, then the collection possibility function c(y) is:

$$\mathrm{c}(y)=\begin{cases}0, & \text{for } y \le l \\ \dfrac{y-l}{u-l}, & \text{for } l < y < u \\ 1, & \text{for } y \ge u\end{cases}$$

Then, the density function of radii of vesicle sections a researcher can get, g(y), is:

$$\mathrm{g}(y)=\frac{\mathrm{c}(y)\,\mathrm{g}(y)}{\int_0^\infty \mathrm{c}(y)\,\mathrm{g}(y)\,\mathrm{d}\,y}$$

With a known r(x), s(y) and g(y) can be calculated using numerical integration. Here I assume r(x) is a log-normal distribution:

$$\mathrm{r}(x)=\frac{1}{x\sigma\sqrt{2\pi}}e^{-\frac{(\ln(x)-\mu)^2}{2\sigma^2}}\text{, for x>0}$$

Now a linear regression can be used to fit μ and σ based on the mean, standard deviation, skewness and kurtosis of actually collected data.

After comparing results obtained through the current method and the simulation method, I found the difference to be around 1%. If the vesicles are much smaller, then the effect of packing will conceivably becomes stronger. The main advantage of the second approach is that it is much faster.

Although developments in design based stereological sampling and computer assisted tomography have brought in promising new methods[24, 25], the traditional approach of taking a random sample slice and quantifying all the observed cross sections of vesicles is still widely used due to limitation of available facility or of sample properties. The main caveat in using such data is to correct the effect of size-biased sampling. Non-parametrical methods for solving this problem have been developed previously[23]. The parametrical method described here is not meant to be a replacement of these existing methods, but rather a simple and efficient way to reach a reasonable estimation.

References

1. Xie Z, Klionsky DJ. Autophagosome formation: core machinery and adaptations. Nat Cell Biol 2007; 9:1102-9.

2. Wang C-W, Stromhaug PE, Shima J, Klionsky DJ. The Ccz1-Mon1 protein complex is required for the late step of multiple vacuole delivery pathways. J Biol Chem 2002; 277:47917-27.

3. Wang C-W, Stromhaug PE, Kauffman EJ, Weisman LS, Klionsky DJ. Yeast homotypic vacuole fusion requires the Ccz1-Mon1 complex during the tethering/docking stage. J Cell Biol 2003; 163:973-85.

4. Bonifacino JS, Glick BS. The mechanisms of vesicle budding and fusion. Cell 2004; 116:153-66.

5. Stagg SM, LaPointe P, Balch WE. Structural design of cage and coat scaffolds that direct membrane traffic. Curr Opin Struct Biol 2007; 17:221-8.

6. Kovacs AL, Palfia Z, Rez G, Vellai T, Kovacs J. Sequestration revisited: integrating traditional electron microscopy, de novo assembly and new results. Autophagy 2007; 3:655-62.

7. Xie Z, Nair U, Klionsky DJ. Atg8 controls phagophore expansion during autophagosome formation. Mol. Biol. Cell. 2008.

8. Ichimura Y, Kirisako T, Takao T, Satomi Y, Shimonishi Y, Ishihara N, Mizushima N, Tanida I, Kominami E, Ohsumi M, Noda T, Ohsumi Y. A ubiquitin-like system mediates protein lipidation. Nature 2000; 408:488-92.

9. Paz Y, Elazar Z, Fass D. Structure of GATE-16, membrane transport modulator and mammalian ortholog of autophagocytosis factor Aut7p. J Biol Chem 2000; 275:25445-50.

10. Nakatogawa H, Ichimura Y, Ohsumi Y. Atg8, a ubiquitin-like protein required for autophagosome formation, mediates membrane tethering and hemifusion. Cell 2007; 130:165-78.

11. Kirisako T, Baba M, Ishihara N, Miyazawa K, Ohsumi M, Yoshimori T, Noda T, Ohsumi Y. Formation process of autophagosome is traced with Apg8/Aut7p in yeast. J Cell Biol 1999; 147:435-46.

12. Kabeya Y, Mizushima N, Ueno T, Yamamoto A, Kirisako T, Noda T, Kominami E, Ohsumi Y, Yoshimori T. LC3, a mammalian homologue of yeast Apg8p, is localized in autophagosome membranes after processing. EMBO J 2000; 19:5720-8.

13. Shintani T, Huang W-P, Stromhaug PE, Klionsky DJ. Mechanism of cargo selection in the cytoplasm to vacuole targeting pathway. Dev Cell 2002; 3:825-37.

14. Pankiv S, Clausen TH, Lamark T, Brech A, Bruun JA, Outzen H, Overvatn A, Bjorkoy G, Johansen T. p62/SQSTM1 binds directly to Atg8/LC3 to facilitate degradation of ubiquitinated protein aggregates by autophagy. J Biol Chem 2007; 282:24131-45.

15. Milenkovic VJ. Position-Based Physics: Simulating the Motion of Many Highly Interacting Spheres and Polyhedra. International Conference on Computer Graphics and Interactive Techniques: Proceedings of the 23rd annual conference on Computer graphics and interactive techniques, 1996:129-36.

16. Lederkremer GZ, Cheng Y, Petre BM, Vogan E, Springer S, Schekman R, Walz T, Kirchhausen T. Structure of the Sec23p/24p and Sec13p/31p complexes of COPII. Proc Natl Acad Sci U S A 2001; 98:10704-9.

17. Kuma A, Mizushima N, Ishihara N, Ohsumi Y. Formation of the approximately 350-kDa Apg12-Apg5.Apg16 multimeric complex, mediated by Apg16 oligomerization, is essential for autophagy in yeast. J Biol Chem 2002; 277:18619-25.

18. Kim J, Huang W-P, Klionsky DJ. Membrane recruitment of Aut7p in the autophagy and cytoplasm to vacuole targeting pathways requires Aut1p, Aut2p, and the autophagy conjugation complex. J Cell Biol 2001; 152:51-64.

19. Suzuki K, Kirisako T, Kamada Y, Mizushima N, Noda T, Ohsumi Y. The pre-autophagosomal structure organized by concerted functions of APG genes is essential for autophagosome formation. Embo J 2001; 20:5971-81.

20. Hanada T, Noda NN, Satomi Y, Ichimura Y, Fujioka Y, Takao T, Inagaki F, Ohusmi Y. The ATG12-ATG5 conjugate has a novel e3-like activity for protein lipidation in autophagy. J Biol Chem 2007.

21. Suzuki K, Kubota Y, Sekito T, Ohsumi Y. Hierarchy of Atg proteins in pre-autophagosomal structure organization. Genes Cells 2007; 12:209-18.

22. Fujita N, Itoh T, Omori H, Fukuda M, Noda T, Yoshimori T. The Atg16L Complex Specifies the Site of LC3 Lipidation for Membrane Biogenesis in Autophagy. Mol. Biol. Cell. 2008; 19:2092-100.

23. Feuerverger A, Menzinger M, Atwood HL, Cooper RL. Statistical methods for assessing the dimensions of synaptic vesicles in nerve terminals. J Neurosci Methods. 2000; 103:181-90.

24. Cruz-Orive LM, Weibel ER. Recent stereological methods for cell biology: a brief survey. Am J Physiol. 1990; 258:L148-56.

25. Geuna S. Appreciating the difference between design-based and model-based sampling strategies in quantitative morphology of the nervous system. J Comp Neurol. 2000; 427:333-9.

Chapter 4
The Release of Atg8 Is Important for Sustaining Autophagosome Formation

Abstract

Eukaryotic cells rely on autophagy to eliminate excess or damaged organelles and proteins. The phagophore assembly site (PAS) is where the core autophagy machinery proteins and their auxiliary factors catalyze the formation of autophagosomes, which are double membrane vesicles carrying cytoplasmic materials for degradation. Although the recruitment of these proteins to the PAS has been extensively studied, little is known about the events happening afterwards or the nature of the PAS. Here we present evidence suggesting that the PAS contains a persistent complex that is used in consecutive rounds of autophagosome formation. Arresting the existing autophagosome formation process by blocking Atg8 release prevents the initiation of new ones. Our data also indicate that the retrograde trafficking of Atg9 from the PAS to peripheral sites happens before the release of Atg8 from the PAS. Blocking the release of Atg8 does not affect the trafficking of Atg9. Conversely, blocking Atg9 departure from the PAS prevents the release of Atg8. Finally, we show that deconjugation of Atg8 is important for maintaining the normal sub-cellular localization of Atg8.

Introduction

Eliminating excess or damaged organelles and proteins is critical in maintaining the health of eukaryotic cells. Macroautophagy, hereafter referred to as autophagy, is a major pathway in achieving such homeostasis [1, 2]. During autophagy, cytoplasmic materials destined for degradation are sequestered into an expanding membrane sac, the phagophore (also known as the isolation membrane), which matures into a double membrane vesicle, the autophagosome. Each completed autophagosome eventually fuses with a lysosome (or a vacuole, in the case of yeast), leading to the degradation of the inner vesicle and its contents.

A set of core autophagy machinery proteins catalyze the formation of autophagosomes at the phagophore assembly site (PAS, also known as the pre-autophagosomal structure) [1, 3]. Depending on the induction stimuli, the core machinery proteins are supplemented by a varying set of auxiliary proteins that modulate the specificity and the magnitude of autophagy. Even though most core machinery proteins are excluded from the completed autophagosomes, it is not clear what happens to the PAS afterwards: whether the PAS retains a basic complex for consecutive rounds of autophagosome formation or the PAS is then completely disassembled.

Among the core machinery proteins, two are known to depart from the PAS during autophagosome formation [4, 5]. One is Atg9, a transmembrane protein. Atg9 localizes to the PAS and non-PAS peripheral sites, including the mitochondria [4, 6-8]. The cycling of Atg9 between the PAS and non-PAS sites has been proposed to be important for the transportation of membrane to the phagophore. Reducing the anterograde trafficking of Atg9 to the PAS results in reduced number of autophagosomes, although their sizes are normal [9]. The departure of Atg9 from the PAS involves the Atg1 complex and the Atg2-Atg18 complex [4]. The other one is Atg8, a ubiquitin-like protein [10, 11]. Unlike most ubiquitin-like proteins, the conjugation target of Atg8 is phosphatidylethanolamine (PE), a lipid. Atg8—PE localizes to the phagophore and controls the sizes of autophagosomes [5, 12-14]. Presumably, after the phagophore is fully expanded, most Atg8 is released to the cytosol by deconjugation[5].

The conjugation and deconjugation of Atg8 involves a set of enzymes. After synthesis, Atg8 is processed by a cysteine protease, Atg4, at the carboxyl terminus, to expose the glycine residue for conjugation [10, 15-17]. The resulted form is termed Atg8ΔR in yeast, since the residue cleaved off is an arginine. The conjugation of Atg8ΔR to PE is catalyzed by the E1-like activating enzyme Atg7, the E2-like conjugation enzyme Atg3, and a possible E3-like protein complex composed of Atg12—Atg5-Atg16, in which Atg12 is conjugated to Atg5. Atg16 in the E3 complex has been shown to determine the membrane target of Atg8 conjugation [10, 18-26]. The deconjugation of Atg8—PE is catalyzed by the same protease, Atg4, which revert Atg8—PE back to Atg8ΔR. If Atg8 is synthesized directly as Atg8ΔR, the conjugation can proceed normally without Atg4.

In this study, we focused on the physiological importance of Atg8 release and the temporal dissection of the autophagosome formation process.

Results

The Release of Atg8 is Necessary for the Regeneration of the PAS

At present, it is not clear what happens to a PAS after the completion of an autophagosome. Does the PAS move on to engage in the next round of autophagosome formation? Or does the existing PAS disassemble and a new PAS reassemble from scratch for each round of autophagosome formation? The two possibilities can be distinguished by arresting the existing autophagosome formation processes (Figure 4.1A). If new rounds of autophagosome formation need the PAS to be freed from prior work, arresting the existing ones will prevent new processes from happening. If a PAS is reassembled from scratch in each round, arresting the existing ones will not immediately affect the formation of the new ones. Instead, new PAS will keep on forming until the essential components are depleted.

We examined the effects of arresting existing autophagosome formation processes by blocking Atg8 deconjugation. In wild type yeast cells, induction of autophagy by starvation leads to sustained production of autophagosomes, as indicated by the

emergence and disappearance of GFP-Atg8 puncta (Figure 4.1B). On average, GFP-Atg8 puncta emerged at a rate of 2~3 per 15 minutes. In contrast, in cells defective in Atg8 deconjugation (*atg4Δ atg8Δ* cells expressing GFP-Atg8ΔR), the frequent emergence of new punta was not observed (Figure 4.1C), suggesting that defect in releasing Atg8 not only arrests the existing autophagosome formation process, but also prevents the initiation of new processes.

The lack of new GFP-Atg8-containing PAS can be explained by a defect in regeneration of the PAS, but can also be explained if deconjugation has dual roles, in both the recruitment of Atg8 to the PAS and its release afterwards. In the latter possibility, a severe kinetic defect in the recruitment may still allow Atg8 to eventually arrive at the PAS that are formed previously, although there might be a significant number of newly formed PAS that do not contain Atg8. To rule out this alternative explanation, we tested whether Atg8 can be recruited normally to newly formed PAS. Atg11 is a protein critical for PAS formation in nutrient-rich condition, but not essential for starvation-induced autophagy [27, 28]. When observed immediately after shifted to starvation medium, most *atg11Δ* cells contained no GFP-Atg8 puncta, indicating that these cells lacked PAS initially (data not shown). After about 30 minutes of incubation, however, GFP-Atg8 puncta started to appear in these cells, indicating that Atg8 was recruited to newly assembled PAS (Figure 4.2A). We then examined *atg11Δ* cells with defect in Atg8 deconjugation. Interestingly, new GFP-Atg8 puncta also appeared in these cells after 30 minutes of starvation (Figure 4.2B). These results suggest that deconjugation primarily affects the release of Atg8 from the PAS, not the recruitment of Atg8 to the PAS.

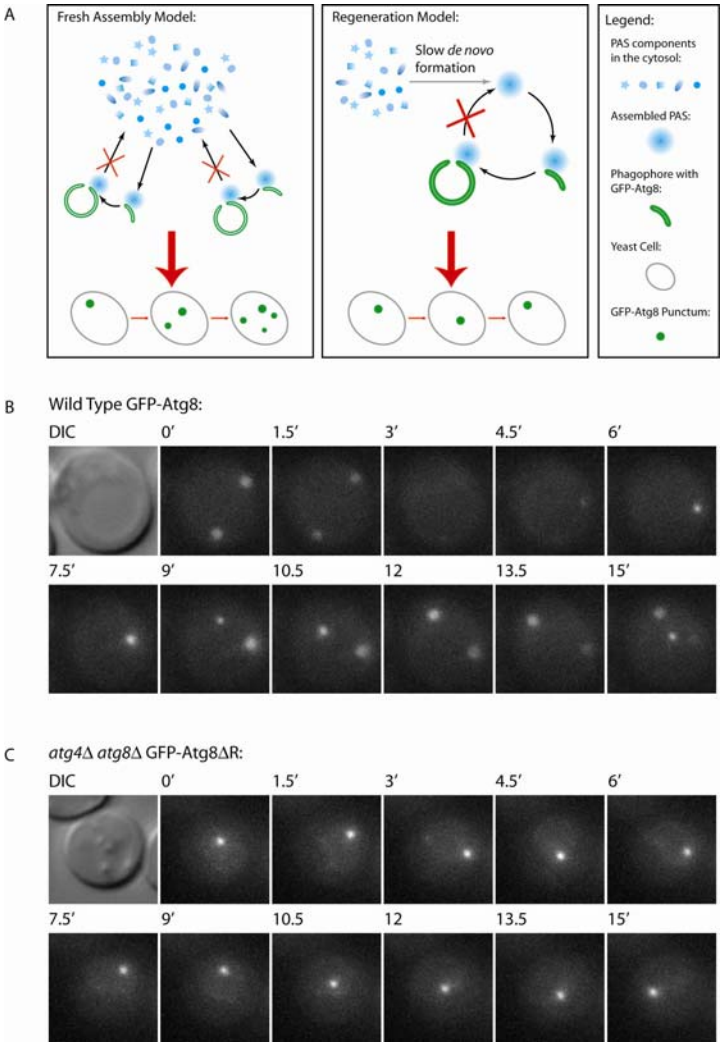

Figure 4.1 The defect in release of Atg8 prevents the regeneration of the PAS

(A) Two potential fates of a PAS after autophagosome formation have different predicted outcomes. As shown in the left panel, one possible model is that a PAS is re-assembled from scratch for each round of autophagosome formation and disassembled afterwards. In this case, arresting existing autophagosome formation processes will not prevent the formation of new PAS until essential components are depleted. Alternatively, the *de novo* formation of the PAS is a slow process; and once formed, the PAS is re-used in consecutive rounds of autophagosome formation. In this model, arresting existing autophagosome formation processes will prevent the initiation of new processes due to lack of an available PAS. (B) New autophagosome formation processes are initiated continuously in wild type cells. Wild type cells expressing GFP-Atg8 were starved for 1 hour, immobilized on Concanavalin A-treated cover slips, and incubated in starvation medium on a depression (concave) slide. Image stacks were collected every 90 seconds and projected to a single image. New autophagosome formation processes were initiated constantly, as indicated by the emergence of GFP-Atg8 puncta. The later decrease and the eventual disappearance of fluorescence signal represent the release of Atg8 and the fusion of the autophagosome with the vacuole. (C) Deconjugation defective cells are unable to initiate new autophagosome formation processes. *atg4Δ atg8Δ* cells expressing GFP-Atg8ΔR were observed as in (B). These cells lacked the frequent emergence of new GFP-Atg8 puncta seen in wild type cells.

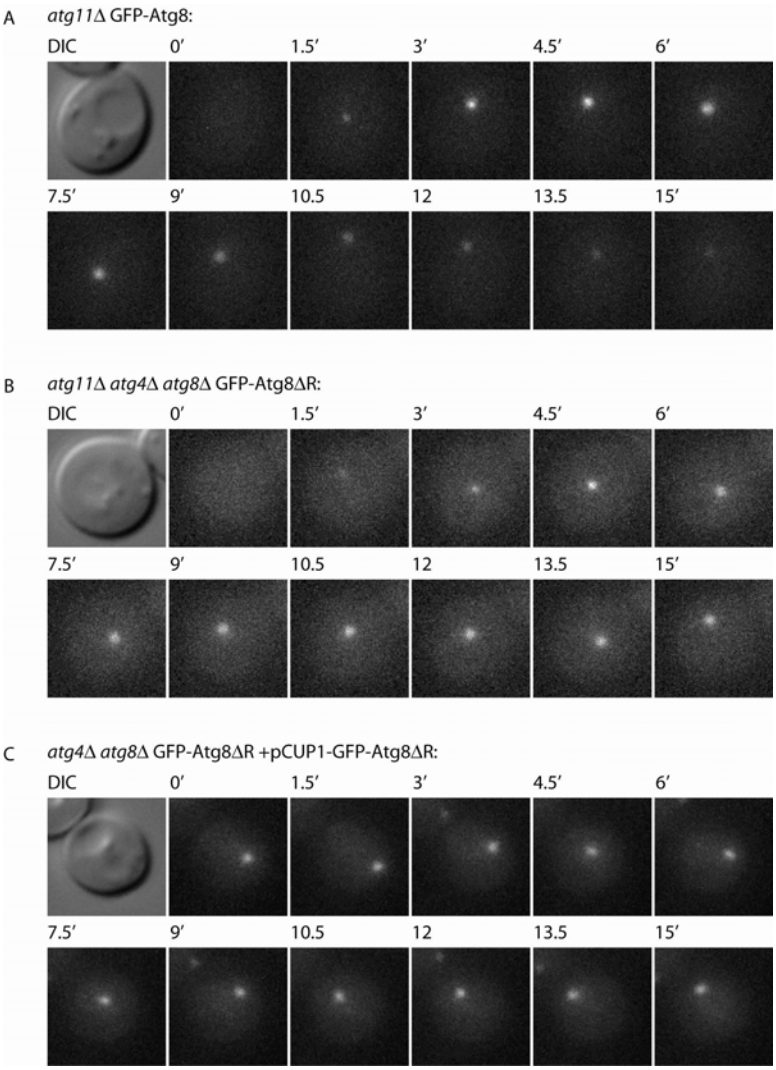

Figure 4.2 The lack of new GFP-Atg8-containing PAS in the absence of Atg8 release is caused by the lack of an available PAS

Fluorescence microscopy was performed as in Figure 4.1B. (A) GFP-Atg8 is recruited to newly formed PAS after starvation. After incubation is starvation medium for about 30 minutes, new GFP-Atg8 puncta started to emerge in *atg11Δ* cells. (B) Deconjugation is not required for Atg8 recruitment to newly formed PAS. *atg4Δ atg8Δ atg11Δ* cells expressing GFP-Atg8ΔR were starved for 30 minutes. New GFP-Atg8 puncta emerged in these cells as in (A). (C) Overexpressing GFP-Atg8ΔR does not lead to emergence of new GFP-Atg8 puncta. *atg4Δ atg8Δ* cells expressing GFP-Atg8ΔR under the control of *CUP1* promoter were starved for 1 hour. No frequent emergence of new GFP-Atg8 puncta was observed.

In wild type cells, the majority of Atg8 at the PAS is released back into the cytosol upon completion of autophagosome formation[5]. Since the amount of Atg8 recruited to the PAS is limited by the amount of Atg8 available in the cell[5], it is possible that a block in Atg8 release may reduce the cytosolic pool and cause the amount of Atg8

at the PAS to drop below the threshold for detection, even if new PAS is being constructed normally. If this is the case, an additional supply of Atg8 will cancel this effect and allow these PAS to recruit a sufficient amount of Atg8 to be detected. To test this possibility, we over-expressed GFP-Atg8ΔR using *CUP1* promoter. When observed by fluorescence microscopy, although the GFP-Atg8 puncta were brighter, the numbers of GFP-Atg8 puncta in the release-defective cells were not significantly different from those without over-expression. Consistently, emergence of new puncta was generally absent (Figure 4.2C). Taken together, these data suggest that the lack of emergence of Atg8-containing PAS when Atg8 release is defective is not because of slow recruitment kinetics or depletion of cytosolic pool of Atg8; instead it is because the PAS can not be regenerated from arrested existing ones.

The Release of Atg8 Happens After the Departure of Atg9

Previously, our laboratory has discovered that Atg9 cycles between the PAS and non-PAS peripheral sites [4]. Atg9 is required for normal Atg8 recruitment to the PAS [29, 30]. Hence Atg9 presumably arrives at the PAS earlier than Atg8 does. On the other hand, the relative timing of Atg9 departure from the PAS versus that of Atg8 release has not been determined. If the autophagosome formation process involves the sequential progression of the PAS through different stages, arresting an earlier step will prevent late events to happen. So we tested the relationship between the departure of Atg9 and the release of Atg8.

Firstly, we examined the localization of Atg9 tagged with three GFP moieties in the carboxyl terminus (Atg9-3xGFP). In wild type cells, Atg9-3xGFP was observed on multiple puncta (Figure 4.3A). This appearance represents the normal steady state localization of Atg9: some at the PAS, some at peripheral sites. In *atg1Δ* cells, which are defective in Atg9 retrograde trafficking, Atg9-3xGFP was concentrated at one or two puncta that presumably represent the PAS (Figure 4.3A) [4]. Interestingly, in cells defective in Atg8 release, Atg9-3xGFP was present in multiple puncta, similar to that in wild type cells (Figure 4.3A). With the precondition that Atg9 is able to travel to the PAS, such result indicates that Atg9 is able to leave the PAS. We then tested if the precondition is

true in this situation by further knocking out *ATG1*. In Atg8 deconjugation defective cells with *ATG1* knocked out, Atg9-3xGFP became concentrated on a few puncta (Figure 4.3A), suggesting that the deconjugation defect does not prevent the trafficking of Atg9 to the PAS. These data indicate that the bidirectional trafficking of Atg9 does not require the release of Atg8.

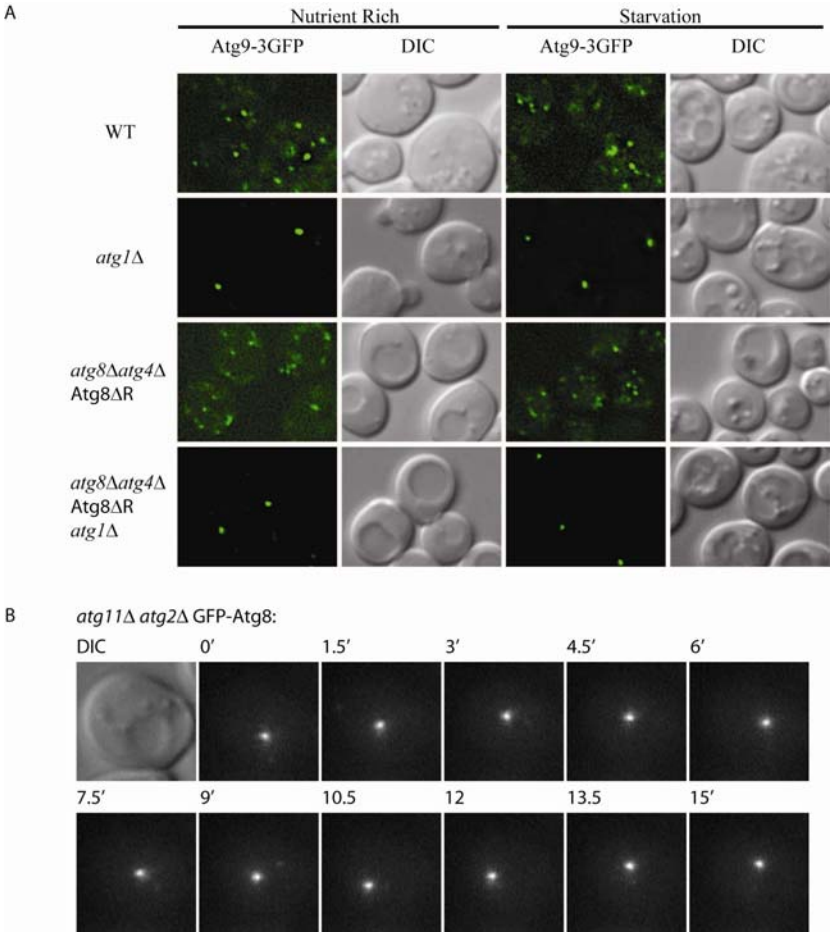

Figure 4.3 The release of Atg8 happens after the departure of Atg9 from the PAS

(A) The trafficking of Atg9 does not depend on the release of Atg8. Cells expressing Atg9-3xGFP were collected from culture growing in rich medium or from culture incubated for 2 hours in starvation medium and observed. A stack of images was taken for each sample, of which one representative image is shown. In wild type cells, Atg9-3xGFP was present at multiple puncta. In *atg1Δ* cells, Atg9-3xGFP was present on one or two puncta. In *atg4Δ atg8Δ* cells expressing Atg8ΔR, Atg9-3xGFP was present on multiple puncta, similar to in wild type cells. In *atg1Δ atg4Δ atg8Δ* cells expressing Atg8ΔR, Atg9-3xGFP was present on one or two puncta per cell. (B) The release of Atg8 depends on the departure of Atg9. *atg2Δ atg11Δ* cells expressing GFP-Atg8 were starved for 1 hour and observed as in Figure 4.1B. Once formed, GFP-Atg8 puncta persisted in these cells.

Next, we tested whether the release of Atg8 depends on the departure of Atg9. For this purpose, we used *atg2Δ atg11Δ* cells. Atg2 interacts with Atg9 and functions in Atg9 departure [4, 31]. We did not choose other genes involved in Atg9 retrograde trafficking, such as *ATG1* and *ATG18*, because they have functions beyond the trafficking of Atg9 [32] (Cao Y. et. al, manuscript in preparation). After shifted to starvation medium, new GFP-Atg8 puncta emerged in these cells (data not shown), indicating that the recruitment of Atg8 to newly formed PAS is normal. In contrast to those dynamic puncta in *atg11Δ* cells, the GFP-Atg8 puncta in *atg2Δ atg11Δ* cells persisted once formed (Figure 4.3B), indicating defect in release. This result suggests that the departure of Atg9 mediated by Atg2 is necessary for the release of Atg8 and implies that the departure of Atg9 happens earlier than the release of Atg8.

Deconjugation of Atg8 Is Important for Maintaining Normal Localization of Atg8

During our examination of the deconjugation defective cells, we noticed an unusual phenomenon: some GFP-Atg8 localizes to the vacuole membrane (Figure 4.4). Compared with cells with other core machinery gene knocked out, deconjugation defective cells have a slightly higher autophagy activity as measured by the Pho8Δ60 assay. In addition, we could see occasional disappearance of GFP-Atg8 puncta in the deconjugation defective cells. So we suspected whether Atg8 molecules on the vacuole membrane arrive there as a result of "leaky" autophagosome formation. If autophagosome can be completed by an alternative albeit slower mechanism without releasing Atg8, the fusion of these unusual autophagosomes will deposit Atg8 on the vacuole limiting membrane. To test this hypothesis, we knocked out *ATG1* and *ATG14* in deconjugation defective cells. Both Atg1 and Atg14 are essential core autophagy machinery proteins [33, 34]. (Their absence completely reduced the autophagy activity in those cells to background level.) Interestingly, the vacuole membrane accumulation of GFP-Atg8 was still present (Figure 4.4), indicating Atg8 reaches vacuole membrane independent of autophagosome formation. Presumably, this population of Atg8 is quickly removed by Atg4 in wild type cells and therefore never observed. This result suggests

that in addition to the E3 complex, active deconjugation by Atg4 is also important for maintaining the correct localization of Atg8—PE.

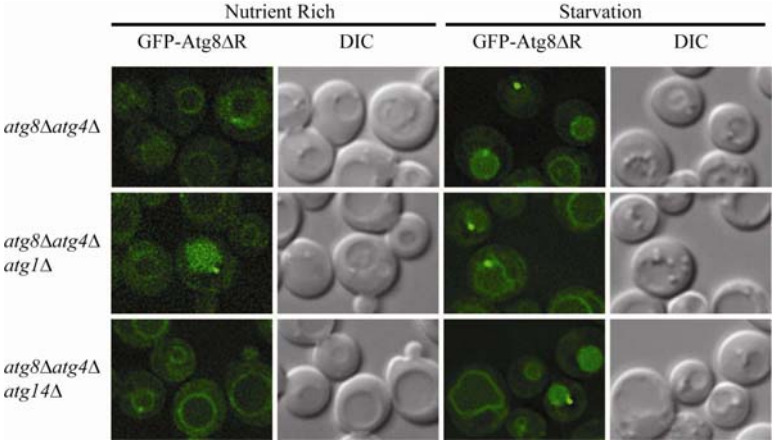

Figure 4.4 Deconjugation is necessary for maintaining normal localization of Atg8

atg4Δ atg8Δ cells expressing GFP-Atg8ΔR were observed as in Figure 4.3A. In addition to the perivacuolar puncta, some GFP-Atg8 was present on the vacuole membrane. Further knocking out *ATG1* or *ATG14* did not abolish the accumulation of GFP-Atg8 on the vacuole membrane.

Discussion

Previously, extensive studies have been carried out to understand the assembly of core autophagy machinery proteins at the PAS. In contrast, little was known about the fate of the PAS after an autophagosome is completed. Here we show that the release of Atg8 from the PAS is necessary for the regeneration of the PAS, suggesting that the PAS contains a persistent basic complex that cycles back to its initial status in order to go through a next round of autophagosome formation. It should be noted that observations in *atg11Δ* background cells clearly demonstrated that the PAS can be formed *de novo*. In order to sustain autophagy, however, the availability of the PAS needs to match the rate of autophagosome formation. On depression slides at room temperature, each wild type cell is producing 2~3 autophagosomes per 15 minutes. In contrast, after 30 minutes of autophagy induction, the PAS is formed in only some *atg11Δ* cells but not all. Therefore the rate of *de novo* formation is insufficient for the high rate of autophagosome formation and the majority of the PAS involved need to come from regeneration.

After the release of Atg8 from the PAS is discovered, determining the relative timing between its release and the retrograde movement of Atg9 becomes a natural next step. Here we showed that the bi-direction movement of Atg9 does not depend on the release of Atg8, whereas the release of Atg8 is blocked when Atg9 retrograde movement is defective. The results suggest that the departure of Atg9 happens earlier than release of Atg8.

The complex of Atg12—Atg5-Atg16 has recently been proposed to function as an E3-like enzyme that specifies the target membrane of Atg8 conjugation [24, 25]. Our data indicate that maintaining correct localization also involves deconjugation. Presumably, the conjugation of Atg8 to the phagophore benefits from enhanced local conjugation activity due to the presence of the E3 complex. Conversely, the lack of E3 complex at other membranes means the conjugation rate will be lower than the rate of deconjugation, preventing mis-localization of Atg8.

Experimental Procedures

Construction of Plasmids and Yeast Strains

Plasmid p1K-GFP-Atg8-406 and pAtg9-PG5 were described previously [5, 35]. These two plasmids express GFP-Atg8 and Atg9-3xGFP under their endogenous promoters. Plasmid p1K-Atg8-404 contains the ATG8 open reading frame with 1 kb of 5' upstream sequence and 200 bp of 3' downstream sequence. The corresponding constructs lacking the last Arginine residue were created by site directed mutagenesis using the following primers: (1) Atg8ΔR Nhe1 PF: ACATTTGGCtaGcAGTCTTTTATATG, and (2) Atg8ΔR Nhe1 PR: AGACTgCtaGCCAAATGTATTTTCTC. The GFP-Atg8ΔR overexpression plasmid pCu-GFP-Atg8ΔR-406 was created by replacing the endogenous promoter with that of 250 bp of *CUP1* 5' sequence. When necessary, the auxotrophic marker genes in these plasmids were swapped using enzyme PvuI. These plasmids were integrated into yeast strains at the locus of the corresponding auxotrophic marker genes. Gene knockouts were performed using standard PCR based approach [36, 37].

Table 4.1 Strains used in this study

Strain Name	Genotype	Reference
TN124	MATα *leu2-3,112 trp1 ura3-52 pho8::pho8Δ60 pho13::LEU2*	[38]
SEY6210	MATα *ura3-52 leu2-3,112 his3-Δ200 trp1-Δ901 lys2-801 suc2-Δ9 mel GAL*	[39]
UNY3	TN121 *atg1Δ*	[32]
YTS153	SEY6210 *atg2Δ::HIS5(S.p.) atg11Δ::LEU2(K.l.)*	This study
YZX275	TN124 *GFP-ATG8::URA3*	This study
YZX284	TN124 *atg4Δ atg8Δ GFP-Atg8ΔR::TRP1*	This study
YZX293	TN124 *atg4Δ atg8Δ Atg8ΔR::TRP1*	This study
YZX295	TN124 *atg4Δ atg8Δ Atg8ΔR::TRP1 Atg9-3xGFP::URA3*	This study
YCY62	TN124 *atg4Δ atg8Δ Atg8ΔR::TRP1 Atg9-3xGFP::URA3 atg1Δ::Ble*	This study
YZX322	TN124 *atg4Δ atg8Δ GFP-Atg8ΔR::TRP1 atg14Δ::URA3(K.l.)*	This study
YCY47	TN124 *atg4Δ atg8Δ GFP-Atg8ΔR::TRP1 atg1Δ::URA3(K.l.)*	This study

Yeast Media

Rich medium (YPD): 1% yeast extract, 2% peptone, 2% glucose. Nitrogen starvation medium (SD-N): 2% glucose, 0.17% yeast nitrogen base without amino acids and ammonium sulfate.

Fluorescence Microscopy

Live cell fluorescence microscopy was performed as previously described[5]. For time-lapse observations, one side of the cover glass was coated with 1 mg/ml concanavalin A for 5 min, and rinsed with water; 100 μl of yeast cell culture was placed on the treated side for 3 min to immobilize yeast cells on the cover glass; the cover glass was rinsed with water, placed on a concavity slide containing liquid medium and observed under the microscope.

References

1. Xie Z, Klionsky DJ. Autophagosome formation: core machinery and adaptations. Nat Cell Biol 2007; 9:1102-9.

2. Mizushima N, Levine B, Cuervo AM, Klionsky DJ. Autophagy fights disease through cellular self-digestion. Nature 2008; 451:1069-75.

3. Yorimitsu T, Klionsky DJ. Autophagy: molecular machinery for self-eating. Cell Death Differ 2005; 12:1542-52.

4. Reggiori F, Tucker KA, Stromhaug PE, Klionsky DJ. The Atg1-Atg13 complex regulates Atg9 and Atg23 retrieval transport from the pre-autophagosomal structure. Dev Cell 2004; 6:79-90.

5. Xie Z, Nair U, Klionsky DJ. Atg8 controls phagophore expansion during autophagosome formation. Mol. Biol. Cell. 2008.

6. Reggiori F, Shintani T, Nair U, Klionsky DJ. Atg9 cycles between mitochondria and the pre-autophagosomal structure in yeasts. Autophagy 2005; 1:101-9.

7. Young ARJ, Chan EYW, Hu XW, Kochl R, Crawshaw SG, High S, Hailey DW, Lippincott-Schwartz J, Tooze SA. Starvation and ULK1-dependent cycling of mammalian Atg9 between the TGN and endosomes. J Cell Sci 2006; 119:3888-900.

8. Yamada T, Carson AR, Caniggia I, Umebayashi K, Yoshimori T, Nakabayashi K, Scherer SW. Endothelial nitric-oxide synthase antisense (NOS3AS) gene encodes an autophagy-related protein (APG9-like2) highly expressed in trophoblast. J. Biol. Chem. 2005; 280:18283-90.

9. Yen W-L, Legakis JE, Nair U, Klionsky DJ. Atg27 is required for autophagy-dependent cycling of Atg9. Mol. Biol. Cell. 2007; 18:581-93.

10. Ichimura Y, Kirisako T, Takao T, Satomi Y, Shimonishi Y, Ishihara N, Mizushima N, Tanida I, Kominami E, Ohsumi M, Noda T, Ohsumi Y. A ubiquitin-like system mediates protein lipidation. Nature 2000; 408:488-92.

11. Paz Y, Elazar Z, Fass D. Structure of GATE-16, membrane transport modulator and mammalian ortholog of autophagocytosis factor Aut7p. J. Biol. Chem. 2000; 275:25445-50.

12. Kirisako T, Baba M, Ishihara N, Miyazawa K, Ohsumi M, Yoshimori T, Noda T, Ohsumi Y. Formation process of autophagosome is traced with Apg8/Aut7p in yeast. J. Cell Biol. 1999; 147:435-46.

13. Kabeya Y, Mizushima N, Ueno T, Yamamoto A, Kirisako T, Noda T, Kominami E, Ohsumi Y, Yoshimori T. LC3, a mammalian homologue of yeast Apg8p, is localized in autophagosome membranes after processing. EMBO J 2000; 19:5720-8.

14. Kabeya Y, Mizushima N, Yamamoto A, Oshitani-Okamoto S, Ohsumi Y, Yoshimori T. LC3, GABARAP and GATE16 localize to autophagosomal membrane depending on form-II formation. J Cell Sci 2004; 117:2805-12.

15. Kirisako T, Ichimura Y, Okada H, Kabeya Y, Mizushima N, Yoshimori T, Ohsumi M, Takao T, Noda T, Ohsumi Y. The reversible modification regulates the membrane-binding state of Apg8/Aut7 essential for autophagy and the cytoplasm to vacuole targeting pathway. J. Cell Biol. 2000; 151:263-76.

16. Hemelaar J, Lelyveld VS, Kessler BM, Ploegh HL. A single protease, Apg4B, is specific for the autophagy-related ubiquitin-like proteins GATE-16, MAP1-LC3, GABARAP, and Apg8L. J. Biol. Chem. 2003; 278:51841-50.

17. Tanida I, Sou YS, Ezaki J, Minematsu-Ikeguchi N, Ueno T, Kominami E. HsAtg4B/HsApg4B/autophagin-1 cleaves the carboxyl termini of three human Atg8 homologues and delipidates microtubule-associated protein light chain 3- and GABAA receptor-associated protein-phospholipid conjugates. J. Biol. Chem. 2004; 279:36268-76.

18. Mizushima N, Noda T, Yoshimori T, Tanaka Y, Ishii T, George MD, Klionsky DJ, Ohsumi M, Ohsumi Y. A protein conjugation system essential for autophagy. Nature 1998; 395:395-8.

19. Tanida I, Tanida-Miyake E, Ueno T, Kominami E. The human homolog of *Saccharomyces cerevisiae* Apg7p is a Protein-activating enzyme for multiple substrates including human Apg12p, GATE-16, GABARAP, and MAP-LC3. J. Biol. Chem. 2001; 276:1701-6.

20. Kuma A, Mizushima N, Ishihara N, Ohsumi Y. Formation of the approximately 350-kDa Apg12-Apg5.Apg16 multimeric complex, mediated by Apg16 oligomerization, is essential for autophagy in yeast. J. Biol. Chem. 2002; 277:18619-25.

21. Tanida I, Tanida-Miyake E, Komatsu M, Ueno T, Kominami E. Human Apg3p/Aut1p homologue is an authentic E2 enzyme for multiple substrates, GATE-16, GABARAP, and MAP-LC3, and facilitates the conjugation of hApg12p to hApg5p. J. Biol. Chem. 2002; 277:13739-44.

22. Mizushima N, Kuma A, Kobayashi Y, Yamamoto A, Matsubae M, Takao T, Natsume T, Ohsumi Y, Yoshimori T. Mouse Apg16L, a novel WD-repeat protein, targets to the autophagic isolation membrane with the Apg12-Apg5 conjugate. J Cell Sci 2003; 116:1679-88.

23. Nemoto T, Tanida I, Tanida-Miyake E, Minematsu-Ikeguchi N, Yokota M, Ohsumi M, Ueno T, Kominami E. The mouse *APG10* homologue, an E2-like enzyme for Apg12p conjugation, facilitates MAP-LC3 modification. J. Biol. Chem. 2003; 278:39517-26.

24. Hanada T, Noda NN, Satomi Y, Ichimura Y, Fujioka Y, Takao T, Inagaki F, Ohusmi Y. The ATG12-ATG5 conjugate has a novel e3-like activity for protein lipidation in autophagy. J. Biol. Chem. 2007.

25. Fujita N, Itoh T, Omori H, Fukuda M, Noda T, Yoshimori T. The Atg16L Complex Specifies the Site of LC3 Lipidation for Membrane Biogenesis in Autophagy. Mol. Biol. Cell. 2008; 19:2092-100.

26. Mizushima N, Sugita H, Yoshimori T, Ohsumi Y. A new protein conjugation system in human. The counterpart of the yeast Apg12p conjugation system essential for autophagy. J. Biol. Chem. 1998; 273:33889-92.

27. Kim J, Kamada Y, Stromhaug PE, Guan J, Hefner-Gravink A, Baba M, Scott SV, Ohsumi Y, Dunn WA, Jr., Klionsky DJ. Cvt9/Gsa9 functions in sequestering selective cytosolic cargo destined for the vacuole. J. Cell Biol. 2001; 153:381-96.

28. Shintani T, Klionsky DJ. Cargo proteins facilitate the formation of transport vesicles in the cytoplasm to vacuole targeting pathway. J. Biol. Chem. 2004; 279:29889-94.

29. Suzuki K, Kirisako T, Kamada Y, Mizushima N, Noda T, Ohsumi Y. The pre-autophagosomal structure organized by concerted functions of *APG* genes is essential for autophagosome formation. EMBO J 2001; 20:5971-81.

30. Suzuki K, Kubota Y, Sekito T, Ohsumi Y. Hierarchy of Atg proteins in pre-autophagosomal structure organization. Genes Cells 2007; 12:209-18.

31. Wang C-W, Kim J, Huang W-P, Abeliovich H, Stromhaug PE, Dunn WA, Jr., Klionsky DJ. Apg2 is a novel protein required for the cytoplasm to vacuole targeting, autophagy, and pexophagy pathways. J. Biol. Chem. 2001; 276:30442-51.

32. Cheong H, Nair U, Geng J, Klionsky DJ. The Atg1 Kinase Complex Is Involved in the Regulation of Protein Recruitment to Initiate Sequestering Vesicle Formation for Nonspecific Autophagy in *Saccharomyces cerevisiae*. Mol. Biol. Cell. 2008; 19:668-81.

33. Tsukada M, Ohsumi Y. Isolation and characterization of autophagy-defective mutants of *Saccharomyces cerevisiae*. FEBS Lett 1993; 333:169-74.

34. Kametaka S, Okano T, Ohsumi M, Ohsumi Y. Apg14p and Apg6/Vps30p form a protein complex essential for autophagy in the yeast, *Saccharomyces cerevisiae*. J. Biol. Chem. 1998; 273:22284-91.

35. Monastyrska I, He C, Geng J, Hoppe AD, Li Z, Klionsky DJ. Arp2 links autophagic machinery with the actin cytoskeleton. Mol. Biol. Cell. 2008; 19:1962-75.

36. Longtine MS, McKenzie A, 3rd, Demarini DJ, Shah NG, Wach A, Brachat A, Philippsen P, Pringle JR. Additional modules for versatile and economical PCR-based gene deletion and modification in *Saccharomyces cerevisiae*. Yeast 1998; 14:953-61.

37. Gueldener U, Heinisch J, Koehler GJ, Voss D, Hegemann JH. A second set of loxP marker cassettes for Cre-mediated multiple gene knockouts in budding yeast. Nucleic Acids Res. 2002; 30:e23.

38. Noda T, Matsuura A, Wada Y, Ohsumi Y. Novel system for monitoring autophagy in the yeast *Saccharomyces cerevisiae*. Biochem Biophys Res Commun 1995; 210:126-32.

39. Robinson JS, Klionsky DJ, Banta LM, Emr SD. Protein sorting in *Saccharomyces cerevisiae*: isolation of mutants defective in the delivery and processing of multiple vacuolar hydrolases. Mol Cell Biol 1988; 8:4936-48.

Chapter 5
Conclusions and Perspectives

Brief Summary of Results

The formation of autophagosomes is morphologically and functionally the central part of the autophagy pathway. Previous studies have gradually discovered the order of assembly of the core machinery proteins at the PAS. In contrast, we know little about what these proteins do after PAS assembly. In this study, I first focused on how Atg8 function in autophagosome formation and demonstrated that (1) the amount of Atg8 at the PAS control the size of autophagosomes produced and that (2) each round of autophagosome formation involves the recruitment of Atg8 to the phagophore and the deconjugation and release of Atg8 from the phagophore. In my study, I have established a temporal dissection of autophagosome formation process based on time-lapse observation of live cells. The temporal dissection extended the effectiveness of fluorescence microscopy beyond studying the PAS assembly and allowed examination of events at late stages of autophagosome formation. This led to the further discovery that the defects in Atg8 release not only arrest the existing autophagosome formation processes, but also prevent the regeneration of the PAS, which is necessary for sustained autophagosome formation. In addition, the data suggest that the release of Atg8 happens after the departure of Atg9 from the PAS, and that deconjugation of Atg8 is important in maintaining correct localization of Atg8.

In an attempt to estimate the area density of Atg8 on the phagophore, I developed two statistical methods for calculating the sizes of intracellular vesicles from sizes of their sections obtained through transmission electron microscopy. Both methods rely on

establishing the correlation of section size distribution with vesicle size distribution, which is then used to calculate the parameters of vesicle size distribution from collected section size data. The first method uses computer programming to simulate the random section of vesicles and take into consideration the effect of vesicle (autophagic bodies) aggregation. The second method takes a faster numerical integration approach that ignores the aggregation effect. Unlike existing analytical solutions, both methods free users from dealing with complex differential equations. The second method may appeal to more potential users since it only requires acquaintance with Microsoft Excel.

Perspectives

Function of Atg8

Even though Atg8 has long been known as a ubiquitin-like protein, their functional analogy seems to be limited to the conjugation reaction. After conjugation, ubiquitinated proteins are often regulated by various types of ubiquitin-binding proteins. In contrast, the list of proteins which interacts with Atg8—PE is very short, as it only contains Atg4 and Atg19. Atg4 is the de-conjugation enzyme. Atg19 is a cargo receptor. Recent genome-wide protein interaction studies identified two potential interacting partners: Atp14 and Crc1. Both Atp14 and Crc1 are mitochondrial inner membrane proteins, casting doubts on their physiological relevance. So, are we at the end of the story? Not necessarily. Past genome-wide screenings may have missed the potential target for two reasons. Firstly, instead of forming a stable complex, Atg8 might interact with its partners transiently only at a specific stage or two during autophagosome formation. Most large-scale screenings are carried out using nutrient rich media, in which the autophagy activity is at a low basal level. The transient nature of the interaction combined with low occurrence of autophagosome formation in the cells could have prevented the successful detection. Secondly, when Atg8 is used as the bait in screening, it is generally tagged at the carboxyl-terminus. Should the tagged Atg8 function normally,

the tag would have been cleaved off by Atg4, voiding the original purpose. These two problems can be easily remedied if Atg8 is the focus of research. The tag can be added to the amino-terminus. The cells can be starved. The autophagosome formation process can also be arrested. Atg8 stays at the PAS under at least 3 conditions: when the retrograde movement of Atg9 is blocked, when the kinase activity of Atg1 is inhibited, when the deconjugation of Atg8 is blocked. These modifications should improve the chances of detecting potential Atg8 interacting proteins.

If new interacting partners can be identified, the study of the physiological function of the interaction can benefit from our structural knowledge of Atg8. A typical Atg8 family protein is composed of two domains. One domain is the ubiquitin-fold, which can be aligned to ubiquitin with a Z-score of 6. The other domain is made of the N-terminal residuals, which forms 2 alpha helices covering part of the ubiquitin-fold. The N-terminal domain is unique to the Atg8 family of ubiquitin-like proteins. Interestingly, two independent studies suggest that the N-terminal domain can go through conformational changes in aqueous solution. Such a conformational change could potentially expose a patch of conserved amino acids that is otherwise covered by the N-terminal domain in the crystal structure. Alanine-scan of the surface residues have shown that mutations in or adjacent to the covered area reduce autophagy activity as much as removing the N-terminal domain does. Should this area turn out to be an interaction surface, the function and regulation of the interaction will surely be fascinating research objects.

Temporal and spatial dissection of autophagosome formation

Besides Atg8, how do other core machinery proteins work together to form autophagosomes? For each of these proteins, at least three questions should be answered: what action(s) it performs, where it performs the action, and when it performs the action. Currently, attempts to answer the first question are hindered by our limited ability to decipher the enzymatic activity of a novel protein from its structure. In contrast, we are much better equipped to deal with the latter two: where and when. Specifically, the focus

of "where" is the spatial structure of core machinery proteins and the phagophore at the PAS, and the focus of "when" is the temporal order of the trafficking of the core machinery proteins to, from, and potentially within the PAS. Combining these two aspects together, we will then have a model that describes the re-organization of the spatial structure of the PAS through consecutive stages of autophagosome formation, in coordination with the trafficking of the proteins and the metamorphosis of the phagophore. Our understanding of the functions of these proteins will also benefit from such a model.

The first step into constructing such a model is to establish spatial and temporal reference points. The current model of autophagosome formation was envisioned at a time when little information of the molecular machinery was available. The proposed intermediate stages are largely conceptual. With the knowledge accumulated in the past decade, it is now possible to examine the actual intermediates. Previous studies and my work have indicated that at least two events are happening after the initial assembly of the PAS: the retrograde movement of Atg9 and the release of Atg8. The release of Atg8 presumably happens later. Mutants blocking either event can therefore provide a snapshot of an intermediate stage of autophagosome formation. One approach is to examine the condition of the phagophore, and the localization of Atg9 and Atg8 relative to the phagophore using immuno-EM. It is also possible to use fluorescence microscopy to study the spatial structure if the diameter is larger than 200 nm. The localization of other core machinery proteins can then be compared with that of Atg9, Atg8, or the phagophore. Both Atg8—PE and Atg9 are membrane-associated, one being lipid conjugated, the other a transmembrane protein. The PAS also contains PI3P produced by the autophagy specific PI3K complex, which recruits effector proteins, such as Atg18 and Atg21, to the PAS. It is not known, however, whether Atg8—PE, Atg9, Atg18 and Atg21 reside on the same membrane structure. Resolving the spatial structure of the PAS and the actual intermediates of phagophore will provide new insights into the function of these proteins.

Another method to study the temporal order is live-cell time-lapse fluorescence microscopy. Here, the trafficking pattern of Atg8 serves as a perfect reference. Unlike conventional genetic epistasis analysis that addresses dependency, this approach can

answer the question of timing directly and be applied to trafficking kinetics studies. Furthermore, when analyzing the phenotype of mutants, especially conditional mutants, one can ask how the whole process is affected instead of just how PAS assembly is affected. The main obstacle to this approach is the signal strength of fluorescent proteins relative to the sensitivity of the microscope. The observation of Atg8 is possible because it is the most abundant core machinery protein at the PAS. Signal strengths of other tagged core machinery proteins are much weaker so that in order to get reliable detection, strong photobleaching is unavoidable. The observation of Atg9 trafficking proves to be a different challenge because it resides in numerous small punta moving at high speed that by the time a scan of the whole cell is done, each puctum may have gone through several sections. Considering the fast advance of electronics, this obstacle will soon be overcome when the availability of more sensitive equipments improves. After all, not too long ago we still relied on overexpressed proteins to get a good image.

When referring to autophagosome formation, most people will think about the classical model in which a membrane sac expands and matures into a double membrane vesicle. Even if this conceptual model can gather further supporting data from aforementioned spatial and temporal dissection studies, one should not forget that the same set of core machinery proteins are involved in a morphologically distinct process, micropexophagy. Thanks to the large sizes of the peroxisomes, the spatial organization of the core machinery proteins is much easier to resolve. If macroautophagy process and micropexophagy evolved from a common ancestral form of autophagy, dissecting the micropexophagy process might provide a fast track to the understanding of PAS organization principle. It is interesting to note that in micropexophagy, Atg—PE and Atg9 localize to different membrane structures. Atg8—PE localizes to a special membrane sac (MIPA), whereas Atg9, together with Atg18, localize to the vacuole extensions. If they also reside on different compartments in macroautophagy, it would suggest that two pathways share the same topological organization. Alternatively, if the core machinery proteins were originally utilized in a process different than either pathway and the two autophagic processes later evolved independently, analyzing these two processes together may nevertheless ease the task of deciphering the activities of these proteins, which by themselves are presumably the same, only in different forms. In

general, the study on micropexophagy has not been as extensive as that of macroautophagy, since fewer laboratories are involved. As research in this field is picking up speed in recent years, it might turn into a rich resource for the understanding of core machinery proteins.

5-Year Outlook

The first autophagy specific gene, *ATG1*, was reported in 1993. By 2003, when the nomenclature was unified, the list had already included 27 genes. Based on the existing data, the entire autophagosome formation machinery can be categorized into the core machinery and the auxiliary factors; and the core machinery proteins can be put into several functional groups. In addition, we have a preliminary understanding of the enzymatic activities of several core machinery proteins. As the research in the field deepens, in the next five years, we should be able to establish a basic framework on the spatial and temporal organization of the PAS in autophagosome formation. The discovery of new genes will continue. Considering that yeast only have about 2000 more genes than bacteria, the list of yeast genes functioning at the PAS may be completed in a few years and reach a level of about 100 genes, with about 1/3 essential ones and the rest auxiliary ones (among the currently known 31 genes, about 1/2 are essential). The list in mammals will take longer to exhaust, although most entries will be auxiliary factors fine-tuning the autophagy process. The complete list of core machinery proteins will facilitate the identification of the regulation target of each auxiliary factor and improve our understanding of how autophagy is regulated in physiological or pathological conditions. Because autophagy is a process that affects various aspects of cellular physiology and both inadequate autophagy and excess autophagy are harmful, knowledge on the auxiliary factors will be very important in successful therapeutic manipulation of autophagy so that the autophagy process can occur at the desired timing and location towards the intended targets.